

From Universal Approximation Theorem to Tropical Geometry of Multi-Layer Perceptrons

Yi-Shan Chu^{*1} and Yueh-Cheng Kuo^{†1}

¹Department of Mathematical Sciences, National Chengchi University, Taipei, Taiwan

October 20, 2025

Abstract

We revisit the Universal Approximation Theorem (UAT) through the lens of the tropical geometry of neural networks and introduce a constructive, geometry-aware initialization for sigmoidal multi-layer perceptrons (MLPs). Tropical geometry shows that Rectified Linear Unit (ReLU) networks admit decision functions with a combinatorial structure often described as a tropical rational, namely a difference of tropical polynomials. Focusing on planar binary classification, we design purely sigmoidal MLPs that adhere to the finite-sum format of UAT: a finite linear combination of shifted and scaled sigmoids of affine functions. The resulting models yield decision boundaries that already align with prescribed shapes at initialization and can be refined by standard training if desired. This provides a practical bridge between the tropical perspective and smooth MLPs, enabling interpretable, shape-driven initialization without resorting to ReLU architectures. We focus on the construction and empirical demonstrations in two dimensions; theoretical analysis and higher-dimensional extensions are left for future work.

1 Introduction

Multi-layer perceptrons (MLPs) are a foundational model class with numerous extensions and architectural variants, and they have demonstrated empirical success across artificial intelligence, computer vision, robotics, and beyond. Despite this breadth of applications, our theoretical understanding of MLPs and the connections among different viewpoints remain incomplete.

A classical line of work establishes *existence* results: under mild assumptions on the activation function and with suitable choices of parameters, finite linear combinations of sigmoids of affine forms are dense in natural function spaces. In particular, Cybenko [5] showed that, for a sigmoidal activation σ , functions of the form

$$G(x) = \sum_{j=1}^N \alpha_j \sigma(w_j^\top x + \theta_j), \quad x \in \mathbb{R}^d, \quad (1.1)$$

can approximate any continuous mapping on a compact domain to arbitrary accuracy; subsequent extensions and refinements were provided, e.g., by Hornik [14]. While these universal approximation theorems (UATs) certify *what* can be represented, they do not prescribe *how* to construct such networks for a desired decision set, which limits interpretability and hinders geometry-aware design.

^{*}Corresponding author. Email: easonchu7@gmail.com

[†]Email: kuoyc@nccu.edu.tw

A complementary, more combinatorial perspective comes from the tropical geometry of neural networks. For ReLU models, decision functions admit piecewise-linear descriptions with rich polyhedral structure, and the decision boundary can often be analyzed through a *tropical rational* (a tropical quotient of two tropical polynomials) [1, 3, 31]. This viewpoint highlights explicit boundary programming and dual polyhedral objects (e.g., zonotopes), yet most existing constructions are tailored to ReLU piecewise-linear networks.

In this work, we revisit UAT *through* the tropical lens and develop a constructive, geometry-aware initialization for *sigmoidal* MLPs that retains the finite-sum structure in (1.1). Our approach compiles a geometric covering of a target region into the weights of a purely sigmoidal network, yielding decision boundaries that match the prescribed shape at initialization; subsequent training is optional and serves primarily as refinement. In doing so, we provide a practical bridge from tropical-style boundary reasoning to smooth MLPs within the classical UAT format.

Related work. The universal approximation literature spans several complementary directions. Beyond the earliest sigmoidal results of Cybenko [5] and extensions by Hornik [14], there are alternative proofs and activation assumptions [8, 20], as well as rate and complexity analyses (e.g., Barron-type bounds) [2, 29]. Depth further changes the picture via expressivity and separation phenomena [25, 30], while practical constructive schemes include radial-basis and extreme-learning approaches that select or randomize hidden units and then fit linear output layers [17, 28].

A complementary line analyzes piecewise-linear networks through tropical geometry, where ReLU decision functions inherit polyhedral structure and can be described via *tropical rational* (differences of tropical polynomials) with dual objects such as zonotopes [1, 31]. Recent work investigates parameter spaces and “real tropical” viewpoints that connect continuous families of networks with combinatorial models [3], and explores compression and structure preservation in tropical terms [7].

Our contribution differs in two aspects: (i) we stay entirely within the sigmoidal, finite-sum format of UAT yet construct *geometrically aligned* hidden units with appropriate weights by constructing a finite ball cover of the target region; (ii) we apply the tropical perspective only as a guiding analogy for boundary programming, without relying on ReLU or log-sum-exp mechanisms. This positions our method between constructive approximation and tropical analyses, emphasizing interpretable, shape-driven initialization.

Section 2 recalls the Universal Approximation Theorem (UAT) for sigmoidal multi-layer perceptrons and summarizes the guarantees relevant to our finite-sum construction. Section 3 introduces tropical algebra and the tropical-geometric viewpoint on neural decision functions, providing the terminology used throughout. Section 4 presents a one-dimensional warm-up ($\mathbb{R} \rightarrow \{0, 1\}$) that illustrates the basic cases and how MLPs act. Section 5 develops the planar case with convex target regions and unions of convex sets. Section 6 consider general planar regions and apply an algorithm that compiles a ball cover into the weights of a sigmoidal MLP, together with implementation details and complexity considerations. Section 7 outlines extensions beyond the plane and discusses how the construction adapts in higher dimensions. Section 8 demonstrates applications and case studies using real data. Section 9 concludes with limitations and directions for future work.

2 Universal Approximation for Sigmoidal MLPs

We adopt the classical finite-sum model for single-hidden-layer networks:

$$G_N(x) = \sum_{j=1}^N \alpha_j \sigma(w_j^\top x + \theta_j), \quad x \in \mathbb{R}^d, \quad (2.1)$$

where $N \in \mathbb{N}$, $\alpha_j \in \mathbb{R}$, $w_j \in \mathbb{R}^d$, and $\theta_j \in \mathbb{R}$ are free parameters, and $\sigma : \mathbb{R} \rightarrow \mathbb{R}$ is a fixed activation.

Definition 2.1 (Sigmoidal activation; [5, Def. 1]). A function $\sigma : \mathbb{R} \rightarrow \mathbb{R}$ is called *sigmoidal* if it is bounded and

$$\lim_{t \rightarrow +\infty} \sigma(t) = 1, \quad \lim_{t \rightarrow -\infty} \sigma(t) = 0.$$

Typical examples include the logistic function (sigmoid function) $\sigma(t) = (1 + e^{-t})^{-1}$ and smooth variants such as \tanh (after affine rescaling).

Universal approximation (UAT). Cybenko proved that the class $\{G_N\}_{N \geq 1}$ with a sigmoidal σ is dense in $C(K)$, the continuous real-valued functions on a compact set $K \subset \mathbb{R}^d$, under the uniform norm.

Theorem 2.2 (Cybenko's UAT; [5, Thm. 2]). *Let σ be sigmoidal in the sense of Definition 2.1. Then, for any compact $K \subset \mathbb{R}^d$, the set of finite sums (2.1) is dense in $C(K)$ with respect to the sup norm, i.e., for every $f \in C(K)$ and every $\varepsilon > 0$, there exist N and parameters $\{\alpha_j, w_j, \theta_j\}_{j=1}^N$ such that $\sup_{x \in K} |f(x) - G_N(x)| < \varepsilon$.*

We adopt the classical single-hidden-layer, finite-sum model defined as in (2.1). Subsequent work broadened both the function classes and the activation assumptions. Funahashi established a closely related universality result for continuous mappings on compact sets using analytic arguments [8]. Hornik extended universality beyond uniform approximation on $C(K)$ to vector-valued outputs and to $L^p(\mu)$ spaces, and relaxed activation requirements far beyond the sigmoidal case [14, 15]. A sharp activation criterion was later given by Leshno, Lin, Pinkus, and Schocken, who characterized universality purely in terms of σ [20].

Theorem 2.3 (Nonpolynomial criterion [20, Thm. 3.2]). *Let $K \subset \mathbb{R}^d$ be compact with nonempty interior. The linear span of $\{\sigma(w^\top x + \theta) : w \in \mathbb{R}^d, \theta \in \mathbb{R}\}$ is dense in $C(K)$ if and only if σ is a. e. not a polynomial.*

While these results certify density, they do not quantify rates or provide constructive recipes for choosing the parameters in (2.1). Barron addressed rates by identifying a Fourier-based function class (now called the Barron class) for which there exist networks of the form (2.1) achieving L^2 error of order $O(N^{-1/2})$, with constants independent of input dimension [2]; see also Pinkus [29] for a survey. Beyond function values, Hornik, Stinchcombe, and White showed that networks can approximate a target mapping together with its partial derivatives to arbitrary accuracy under mild smoothness assumptions [16].

These developments establish the expressive power of the finite-sum architecture (2.1) but remain largely nonconstructive regarding *how* to realize a desired decision set. In this paper we remain strictly within the UAT format and propose a geometry-aware procedure that *constructs* the parameters in (2.1) from a prescribed planar region via a ball cover. The resulting sigmoidal networks inherit all classical UAT guarantees by design, while our compilation yields decision boundaries that already align with the target at initialization; training, when used, serves primarily as refinement rather than discovery.

3 Tropical Geometry

Tropical geometry studies algebraic objects after replacing the usual $(+, \times)$ arithmetic by an idempotent, piecewise-linear calculus. Under this correspondence, polynomial equations give rise to polyhedral complexes equipped with rich combinatorics, so that questions from algebraic geometry can be translated into convex- and graph-theoretic statements; see Morrison [26] for a concise introduction and Maclagan and Sturmfels [21] for a comprehensive reference. In this section, we only state some relevant concepts in tropical geometry.

Definition 3.1 (Tropical semiring (max–plus)). The tropical semiring is $\mathbb{T} = \mathbb{R} \cup \{-\infty\}$ with

$$a \oplus b := \max\{a, b\}, \quad a \odot b := a + b,$$

additive identity $-\infty$ and multiplicative identity 0.

Proposition 3.2 (Basic properties of tropical semiring). *Over $(\mathbb{T}, \oplus, \odot)$:*

- (a) \oplus is commutative, associative, and idempotent ($a \oplus a = a$).
- (b) \odot is commutative and associative with identity 0.
- (c) \odot distributes over \oplus : $a \odot (b \oplus c) = (a \odot b) \oplus (a \odot c)$.
- (d) The natural order $a \leq b \iff a \oplus b = b$ coincides with the usual order on \mathbb{R} .

Hence \mathbb{T} is a commutative idempotent semiring (not a ring: \oplus has no additive inverses). [cf. 21, 26]

Remark 3.3 (Min–plus convention). Many texts use the min–plus semiring $(\overline{\mathbb{R}}, \boxplus, \boxtimes)$ with $a \boxplus b = \min\{a, b\}$ and $a \boxtimes b = a + b$, additive identity $+\infty$. It is anti-isomorphic to max–plus via $x \mapsto -x$ [21, 26].

Tropical monomials, polynomials, and hypersurfaces

Definition 3.4. For $u = (u_1, \dots, u_n) \in \mathbb{Z}_{\geq 0}^n$ and $x = (x_1, \dots, x_n) \in \mathbb{T}^n$ we write

$$\langle u, x \rangle := \sum_{i=1}^n u_i x_i,$$

the Euclidean dot product.

Definition 3.5 (Monomials and polynomials). For $x = (x_1, \dots, x_n) \in \mathbb{T}^n$ and $u = (u_1, \dots, u_n) \in \mathbb{Z}_{\geq 0}^n$, the tropical monomial with coefficient $c \in \mathbb{T}$ is $c \odot x^u = c + \langle u, x \rangle$. A *tropical polynomial* is a finite tropical sum

$$F(x) = \bigoplus_{k=1}^m (c_k \odot x^{u^{(k)}}) = \max_{1 \leq k \leq m} \{ c_k + \langle u^{(k)}, x \rangle \}.$$

Remark 3.6 (Tropical powers). For $a \in \mathbb{T}$ and $m \in \mathbb{Z}_{\geq 0}$, the tropical m -th power is the m -fold tropical product

$$a^{\odot m} := \underbrace{a \odot a \odot \cdots \odot a}_{m \text{ times}} = m a \quad (\text{ordinary sum}).$$

For $x = (x_1, \dots, x_n)$ and a multi-index $u = (u_1, \dots, u_n)$ we set

$$x^{\odot u} := x_1^{\odot u_1} \odot \cdots \odot x_n^{\odot u_n} = u_1 x_1 + \cdots + u_n x_n.$$

For convenience we drop the symbol \odot in exponents and write

$$a^u \equiv a^{\odot u}, \quad x^u \equiv x^{\odot u}.$$

With this convention, a tropical monomial with coefficient c can be written as

$$c \odot x^u = c + \langle u, x \rangle.$$

Proposition 3.7 (Convex piecewise-linear structure). *Every tropical polynomial $F : \mathbb{R}^n \rightarrow \mathbb{R}$ can be written as $F(x) = \max_{1 \leq k \leq m} \{c_k + \langle u^{(k)}, x \rangle\}$. Hence F is convex and piecewise-linear with finitely many linear regions, and its set of non-differentiability points equals the corner locus $\mathcal{T}(F)$. [21, 26]*

Example 3.8 (Tropical line in \mathbb{R}^2). Let $F(x, y) = x \oplus y \oplus 0 = \max\{x, y, 0\}$. Then $\mathcal{T}(F)$ is the union of three rays meeting at the origin, with primitive directions $(-1, 0)$, $(0, -1)$, and $(1, 1)$ [26]. See Fig. 1.

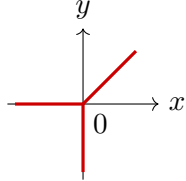


Figure 1: The tropical line $x \oplus y \oplus 0$: three rays at the origin.

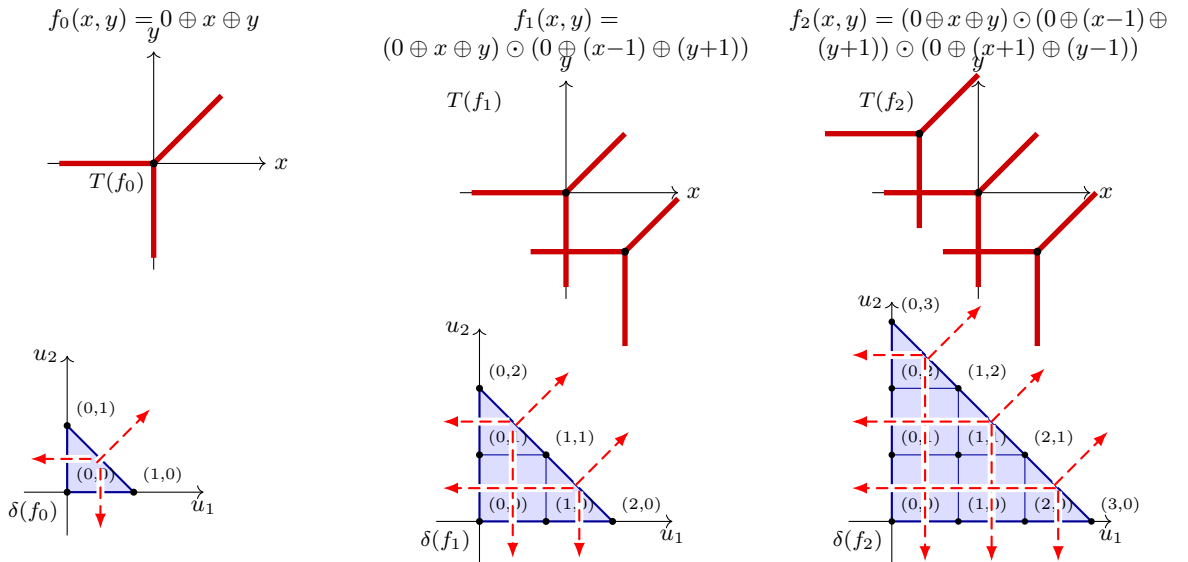


Figure 2: Tropical hypersurfaces $\mathcal{T}(f)$ and subdivision of its Newton polygons $\delta(f)$. Top: $\mathcal{T}(f)$ —unions of 1, 2, and 3 tropical lines (apices $(0, 0)$, $(1, -1)$, $(-1, 1)$). Bottom: $\delta(f)$ —Newton triangles of sizes 1, 2, 3. Red dashed lines are *straight outward primitive normals* (left $(-1, 0)$, bottom $(0, -1)$, diagonal $(1, 1)$), each drawn as a single segment that runs from an interior anchor point, across the edge, and extends outside the polygon.

Definition 3.9. A tropical polynomial is the tropical sum of finitely many monomials,

$$F(x) = \bigoplus_{k=1}^m (c_k \odot x^{\odot u^{(k)}}) = c_1 x^{u^{(1)}} \oplus c_2 x^{u^{(2)}} \oplus \dots \oplus c_m x^{u^{(m)}} = \max_{1 \leq k \leq m} \{c_k + \langle u^{(k)}, x \rangle\}, \quad x \in \mathbb{R}^n.$$

Its *tropical hypersurface* is

$$\begin{aligned} \mathcal{T}(F) &= \left\{ x \in \mathbb{R}^n : |\text{Argmax}_k \{c_k \odot x^{\odot u^{(k)}}\}| \geq 2 \right\} \\ &= \left\{ x \in \mathbb{R}^n : \exists i \neq j \text{ with } c_i \odot x^{\odot u^{(i)}} = c_j \odot x^{\odot u^{(j)}} = F(x) \right\}. \end{aligned}$$

Equivalently, $\mathcal{T}(F)$ is the set of non-differentiability points of the convex piecewise-linear map F . For $n = 2$ it is a tropical curve. [cf. 21, 26]

Definition 3.10. Let $A = \{u^{(1)}, \dots, u^{(m)}\} \subset \mathbb{Z}^n$ be the support of a tropical polynomial F , i.e., $F = \bigoplus_k (c_k \odot x^{u^{(k)}})$. The *Newton polytope* of F is the convex hull of its support A :

$$\text{Newt}(F) := \text{conv}(A) = \text{conv}\{u^{(k)} \in \mathbb{R}^n : c_k \neq -\infty, k = 1, 2, \dots, m\} \subset \mathbb{R}^n.$$

When $n = 2$, $\text{Newt}(F)$ is a lattice polygon. [21, 26]

Definition 3.11 (Upper faces, projection, and dual subdivision). Let

$$F(x) = \bigoplus_{k=1}^m (c_k \odot x^{\odot u^{(k)}}), \quad x \in \mathbb{R}^d,$$

and set $\widehat{A} = \{(u^{(k)}, c_k)\} \subset \mathbb{R}^{d+1}$, $P^\wedge = \text{conv}(\widehat{A})$. Write

$$\text{UF}(P^\wedge) := \{p \subset P^\wedge : p \text{ is a face with an outer normal } \nu \text{ s.t. } \nu_{d+1} > 0\}$$

for the collection of upper faces, and let

$$\pi : \mathbb{R}^d \times \mathbb{R} \longrightarrow \mathbb{R}^d, \quad \pi(v, h) = v$$

be the projection that drops the last coordinate. The *dual subdivision* determined by F is

$$\delta(F) := \{\pi(p) \subset \mathbb{R}^d : p \in \text{UF}(P^\wedge)\}.$$

Then $\delta(F)$ is a polyhedral complex with support $\Delta(F) := \text{Newt}(F) = \text{conv}\{u^{(k)}\}$. By Maclagan and Sturmfels [21, Prop. 3.1.6], the tropical hypersurface $\mathcal{T}(F)$ is the $(d-1)$ -skeleton of the polyhedral complex dual to $\delta(F)$. In particular, each vertex of $\delta(F)$ corresponds to one linearity cell of the convex PL map F , so the number of vertices of $\delta(F)$ upper-bounds the number of linear regions of F .

Theorem 3.12 (Duality Theorem; [21, Prop. 3.1.6]). *Let F be a tropical polynomial on \mathbb{R}^2 and set $P = \text{Newt}(F)$. Let $\delta(F) = \{\pi(p) : p \in \text{UF}(P^\wedge)\}$ be the dual subdivision induced by the coefficients of F (as in Theorem 3.11). Then the tropical curve $\mathcal{T}(F)$ is dual to $\delta(F)$ in the following sense:*

- vertices of $\mathcal{T}(F)$ correspond to polygons in $\delta(F)$;
- edges of $\mathcal{T}(F)$ correspond to interior edges in $\delta(F)$;
- rays of $\mathcal{T}(F)$ correspond to boundary edges of P used by $\delta(F)$;
- regions of \mathbb{R}^2 separated by $\mathcal{T}(F)$ correspond to lattice points of P used in $\delta(F)$.

Moreover, dual edges are orthogonal, adjacency is preserved, and dimensions are reversed.

Tropical rational functions and neural networks

Definition 3.13 (Tropical rational function). Let U, V be tropical polynomials on \mathbb{R}^n . The *tropical rational* function is the classical difference

$$R(x) \equiv U(x) \odot V(x) \equiv U(x) - V(x).$$

Its zero set $\{x : U(x) = V(x)\}$ is a finite union of polyhedral pieces contained in tropical hypersurfaces associated with U and V .

Proposition 3.14. *For tropical polynomials U, V , the decision set $\{x : R(x) \geq 0\}$ coincides with $\{x : U(x) \geq V(x)\}$, and the boundary $\partial\{R \geq 0\}$ is contained in the equality locus $\{x : U(x) = V(x)\} \subset \mathcal{T}(U) \cup \mathcal{T}(V)$. In particular the boundary is a polyhedral complex of dimension $n-1$.*

Proposition 3.15 (ReLU networks as tropical rational maps). *Let $f : \mathbb{R}^n \rightarrow \mathbb{R}$ be the output of a feedforward network with ReLU activations. Then there exist tropical polynomials U, V such that*

$$f(x) = U(x) \oslash V(x).$$

Equivalently, f is a difference of finitely many affine maxima, i.e., $f(x) = (\max_i\{a_i + \langle p_i, x \rangle\}) - (\max_j\{b_j + \langle q_j, x \rangle\})$. Consequently, the linear regions of f form a polyhedral complex, and any binary decision boundary $\{f = 0\}$ is a tropical equality set $U = V$. [see 31]

Proposition 3.15 provides a polyhedral (tropical) model for ReLU networks. In contrast, the constructions developed later remain strictly within the sigmoidal, finite-sum UAT format, yet borrow the “boundary programming” intuition from the tropical viewpoint.

In later sections we compile a ball cover of a target planar region into the weights of a sigmoidal MLP. Although our use is constructive and analytic, unions of balls relate to the *nerve* of a cover; under mild hypotheses, a space is homotopy-equivalent to the nerve of a good cover, providing a combinatorial summary of geometry [24].

4 A one-dimensional warm-up: least-squares construction

In one dimension, we adopt the simplest possible realization that still adheres to the finite-sum UAT template: fix a set of shifts (centers) $p_1, \dots, p_m \in \mathbb{R}$, choose a sigmoidal activation σ , and solve a linear least-squares problem for the output weights. Unlike our 2D construction (Sections 5–6), no tropical reasoning is needed here—everything reduces to a closed-form linear solve.

Model and design matrix. Given data $\{(x_i, y_i)\}_{i=1}^N$ with $x_i \in [a, b] \subset \mathbb{R}$ and $y_i \in \mathbb{R}$, define

$$\Phi(x) = [\sigma(x - p_1), \dots, \sigma(x - p_m), 1]^\top \in \mathbb{R}^{m+1}, \quad \Phi = \begin{bmatrix} \Phi(x_1)^\top \\ \vdots \\ \Phi(x_N)^\top \end{bmatrix} \in \mathbb{R}^{N \times (m+1)}.$$

A single-hidden-layer predictor in the UAT finite-sum form is then $\hat{y}(x) = \Phi(x)^\top \alpha = \sum_{j=1}^m \alpha_j \sigma(x - p_j) + \alpha_{m+1}$.

Closed-form weights. With squared loss, the optimal output weights solve

$$\min_{\alpha \in \mathbb{R}^{m+1}} \|\Phi \alpha - y\|_2^2 \implies \alpha^* = (\Phi^\top \Phi)^{-1} \Phi^\top y,$$

assuming Φ has full column rank. This yields a network that fits the data without any gradient training and stays within the classical UAT format (finite linear combination of shifted/scaled sigmoids of affine inputs).

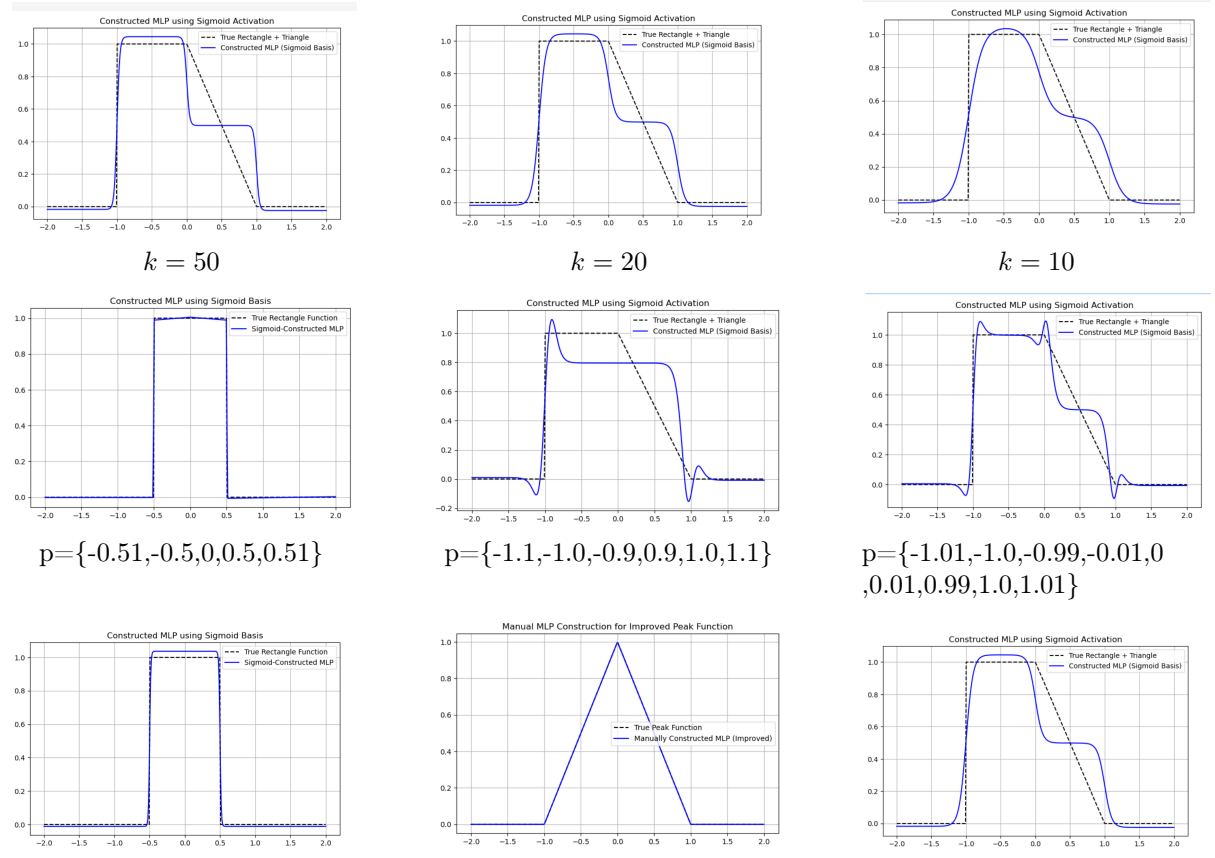
Binary classification outputs. For $\mathbb{R} \rightarrow \{0, 1\}$, one may (i) treat $\hat{y}(x)$ as a probability and threshold at 0.5, or (ii) add a final logistic squashing $p(x) = \sigma(\beta_1 \hat{y}(x) + \beta_0)$ and learn (β_1, β_0) by 1D logistic regression if desired. In our demos we simply threshold \hat{y} .

Algorithm 1 Least-squares 1D initializer (training-free)

Input: Data $\{(x_i, y_i)\}$; centers $\{p_j\}_{j=1}^m$; activation σ

- 1: Build $\Phi \in \mathbb{R}^{N \times (m+1)}$ with $\Phi_{ij} = \sigma(x_i - p_j)$ and a final bias column of ones
- 2: Solve $\alpha^* = (\Phi^\top \Phi)^{-1} \Phi^\top y$
- 3: Define $\hat{y}(x) = \sum_{j=1}^m \alpha_j^* \sigma(x - p_j) + \alpha_{m+1}^*$
- 4: **return** α^* , $\hat{y}(\cdot)$ (optional: threshold at 0.5)

Choice of centers and sharpness. Placing centers $\{p_j\}$ near anticipated breakpoints (e.g., interval endpoints) improves accuracy; more centers increase capacity. A larger sigmoid sharpness k yields sharper transitions at the cost of conditioning—see Fig. 3.



Rectangle function with Sigmoid($k=120$), the given set of points is $\{-0.5, 0.5\}$

Triangle function with ReLU, the given set of points is $\{-1, 0.5, 1\}$

Trapezoid function with Sigmoid($k=20$), the given set of points is $\{-1, 0.5, 1\}$

Figure 3: One-dimensional function fitting with the least-squares initializer. Top row: varying sigmoid sharpness k . Middle row: varying center placements p_j with sigmoid($k=20$). Bottom row: different shapes reconstructed using algorithm 1 without training.

Summary. The 1D case provides a minimal, training-free baseline: once centers are fixed, the network is obtained by a single linear solve. In Section 5 we will abandon least-squares in favor of a geometry-aware compilation on the plane (ball covers and differentiable set operations), which is closer in spirit to tropical analyses of decision boundaries while remaining fully sigmoidal.

5 Planar Convex Regions and Unions

We now give a constructive, geometry-aware initializer for planar binary classification $\mathbb{R}^2 \rightarrow \{0, 1\}$ that stays within the classical finite-sum sigmoidal format (2.1). Geometrically, we approximate a convex target by supporting half-spaces and place steep sigmoid “gates” on those supports; analytically, we *count* the satisfied constraints and threshold; tropically, we view the support stencil as a tropical polynomial whose corner locus prescribes the desired boundary.

Tropical preface. Given outward unit normals $u_\ell \in \mathbb{S}^1$ and supports $h_\ell \in \mathbb{R}$ (one per active side), define the tropical polynomial

$$F(x) = \bigoplus_{\ell=1}^m (h_\ell \odot \langle -u_\ell, x \rangle) = \max_{1 \leq \ell \leq m} \{ h_\ell - \langle u_\ell, x \rangle \}.$$

Its tropical hypersurface $\mathcal{T}(F)$ is orthogonal to the boundary edges of the Newton polygon $\delta(F)$ used by the coefficients, and the set $\{F(x) \geq 0\}$ equals the polytope cut out by the corresponding supports. Our sigmoidal construction below is a smooth relaxation of this hard tropical inequality.

We first recall some basic concepts that are widely used in geometric analysis.

Definition 5.1 (Unit circle \mathbb{S}^1). $\mathbb{S}^1 := \{u \in \mathbb{R}^2 : \|u\|_2 = 1\} = \{(\cos \theta, \sin \theta) : \theta \in [0, 2\pi)\}$. We write $u_\ell \in \mathbb{S}^1$ for outward unit normals to supporting lines of a convex set.

Definition 5.2 (Support function and support values). For a nonempty compact convex set $C \subset \mathbb{R}^2$, its support function is

$$h_C(u) := \sup_{x \in C} \langle u, x \rangle, \quad u \in \mathbb{R}^2.$$

Given a unit outward normal $u_\ell \in \mathbb{S}^1$, the *support value* is $h_\ell := h_C(u_\ell) = \sup_{x \in C} \langle u_\ell, x \rangle$. The supporting line with outward normal u_ℓ is $\{x : \langle u_\ell, x \rangle = h_\ell\}$, and the containing half-space is $\{x : \langle u_\ell, x \rangle \leq h_\ell\}$.

Definition 5.3 (Hausdorff distance). For nonempty compact $A, B \subset \mathbb{R}^2$,

$$d_H(A, B) = \max \left\{ \sup_{a \in A} \inf_{b \in B} \|a - b\|_2, \sup_{b \in B} \inf_{a \in A} \|a - b\|_2 \right\}.$$

Equivalently, $d_H(A, B) = \inf\{\varepsilon \geq 0 : A \subseteq \mathcal{N}_\varepsilon(B), B \subseteq \mathcal{N}_\varepsilon(A)\}$, where $\mathcal{N}_\varepsilon(S) = \{x : \text{dist}(x, S) \leq \varepsilon\}$.

Geometrically, the Hausdorff distance measures how close two sets are. In this paper, we will analyze our construction error with respect to this metric.

Tropical interpretation. Given outward normals $\{u_\ell\}_{\ell=1}^m$ and supports $\{h_\ell\}$, the tropical polynomial

$$F(x) = \bigoplus_{\ell=1}^m (h_\ell \odot x^{-u_\ell}) = \max_{1 \leq \ell \leq m} \{ h_\ell - \langle u_\ell, x \rangle \}$$

has tropical hypersurface $\mathcal{T}(F)$ dual to the subdivision of the Newton polygon $\delta(F)$. The hard set $\{F(x) \geq 0\}$ equals the polytope cut out by the supports.

Polyhedral approximation and Gates. Let $C \subset \mathbb{R}^2$ be compact and convex. Choose outward unit normals $u_\ell \in \mathbb{S}^1$ and support values $h_\ell = h_C(u_\ell)$ so that the polytope

$$C_{\text{poly}} := \bigcap_{\ell=1}^m \{x \in \mathbb{R}^2 : \langle u_\ell, x \rangle \leq h_\ell\} \tag{5.1}$$

approximates C to the desired accuracy in Hausdorff distance. For a sharpness parameter $\kappa > 0$, define the *half-space gates*

$$s_\ell(x) = \sigma(\kappa(h_\ell - \langle u_\ell, x \rangle)), \quad \ell = 1, \dots, m, \tag{5.2}$$

so that $s_\ell(x) \approx 1$ on $\{\langle u_\ell, x \rangle \leq h_\ell\}$ and $s_\ell(x) \approx 0$ otherwise.

Lemma 5.4. Fix $0 < \eta < \frac{1}{2}$ and let $\sigma(t) = \frac{1}{1+e^{-t}}$ be the logistic sigmoid. For a gate $s_\ell(x) = \sigma(\kappa(h_\ell - \langle u_\ell, x \rangle))$ with $\kappa > 0$, define the signed distance to the supporting line by

$$d_\ell(x) := h_\ell - \langle u_\ell, x \rangle.$$

Then the following equivalences hold:

$$s_\ell(x) \geq 1 - \eta \iff d_\ell(x) \geq w_\eta, \quad (5.3)$$

$$s_\ell(x) \leq \eta \iff d_\ell(x) \leq -w_\eta, \quad (5.4)$$

$$\eta \leq s_\ell(x) \leq 1 - \eta \iff |d_\ell(x)| \leq w_\eta, \quad (5.5)$$

where the half-width

$$w_\eta := \frac{1}{\kappa} \log\left(\frac{1-\eta}{\eta}\right).$$

Consequently, the uncertain band (where the gate is not yet close to 0 or 1) around the supporting line $\langle u_\ell, x \rangle = h_\ell$ is the slab $\{x : |d_\ell(x)| \leq w_\eta\}$ of geometric thickness

$$2w_\eta = \frac{2}{\kappa} \log\left(\frac{1-\eta}{\eta}\right) = \Theta(\kappa^{-1}),$$

with constants depending only on η (not on κ).

Proof. Set $z := \kappa d_\ell(x)$. Since σ is strictly increasing, inequalities on $s_\ell(x) = \sigma(z)$ are equivalent to inequalities on z . We use the explicit inverse $\sigma^{-1}(y) = \log\left(\frac{y}{1-y}\right)$.

(i) *High-confidence interior* ($\geq 1 - \eta$).

$$s_\ell(x) \geq 1 - \eta \iff z \geq \sigma^{-1}(1 - \eta) = \log\left(\frac{1-\eta}{\eta}\right) \iff \kappa d_\ell(x) \geq \log\left(\frac{1-\eta}{\eta}\right),$$

which gives (5.3) after dividing by $\kappa > 0$.

(ii) *High-confidence exterior* ($\leq \eta$).

$$s_\ell(x) \leq \eta \iff z \leq \sigma^{-1}(\eta) = \log\left(\frac{\eta}{1-\eta}\right) = -\log\left(\frac{1-\eta}{\eta}\right) \iff \kappa d_\ell(x) \leq -\log\left(\frac{1-\eta}{\eta}\right),$$

which gives (5.4).

(iii) *Transition (uncertain) band.* Combining (i)–(ii),

$$\eta \leq s_\ell(x) \leq 1 - \eta \iff -\log\left(\frac{1-\eta}{\eta}\right) \leq \kappa d_\ell(x) \leq \log\left(\frac{1-\eta}{\eta}\right),$$

equivalently $|d_\ell(x)| \leq w_\eta$, which is (5.5).

The set $\{x : |d_\ell(x)| \leq w_\eta\}$ is a slab of half-width w_η around the line $\langle u_\ell, x \rangle = h_\ell$. Its geometric thickness is therefore $2w_\eta$. Since $\log\left(\frac{1-\eta}{\eta}\right)$ is a positive constant for fixed $\eta \in (0, \frac{1}{2})$, we have $2w_\eta = \Theta(\kappa^{-1})$ as $\kappa \rightarrow \infty$. \square

Remark 5.5 (Other sigmoidal activations). If σ is any strictly increasing sigmoidal activation with continuous inverse on $(0, 1)$, the same proof yields

$$\eta \leq s_\ell(x) \leq 1 - \eta \iff |d_\ell(x)| \leq \frac{1}{\kappa} \max\left\{\sigma^{-1}(1 - \eta), -\sigma^{-1}(\eta)\right\},$$

so the band thickness remains $\Theta(\kappa^{-1})$ with η -dependent constants.

Remark 5.6 (Roles of η and κ). The parameter $\eta \in (0, \frac{1}{2})$ is a *confidence tolerance*: a gate $s_\ell(x) = \sigma(\kappa(h_\ell - \langle u_\ell, x \rangle))$ is *confidently inside* when $s_\ell(x) \geq 1 - \eta$ and *confidently outside* when $s_\ell(x) \leq \eta$. This choice fixes the constant $\log(\frac{1-\eta}{\eta})$ and thus the half-width $w_\eta = \kappa^{-1} \log(\frac{1-\eta}{\eta})$ of the ambiguous strip around each supporting line. In contrast, $\kappa > 0$ is a *sharpness parameter*: increasing κ shrinks the physical band thickness $2w_\eta = \Theta(\kappa^{-1})$, concentrating any classification error into a narrower neighborhood of the boundary. Practically, one may fix a small η (e.g. $10^{-2} \sim 10^{-1}$) to interpret the numerical limit to 0/1, then tune κ to achieve the desired geometric band width. *Equivalently, without the definition of η explicitly, one may target a desired saturation $s_\ell(x) \geq 1 - \epsilon$ at distance t from the boundary and choose $\kappa \geq \frac{1}{t} \log \frac{1-\epsilon}{\epsilon}$.*

Binary classifier on convex sets

Define the *count function*

$$F_{m,\kappa}(x) = \sum_{\ell=1}^m s_\ell(x) = \sum_{\ell=1}^m \sigma(\kappa(h_\ell - \langle u_\ell, x \rangle)),$$

and the baseline threshold $\tau_m := m - \frac{1}{2}$. More generally, writing $\tau = m - \delta$ with $\delta \in (0, 1)$, correct separation is guaranteed whenever

$$m\eta < \delta < 1 - \eta.$$

Intuitively, a larger δ (stricter threshold, τ closer to m) demands a smaller η so interior gates are sufficiently close to 1; a smaller δ (looser threshold) can admit points with an unsatisfied facet unless η is also reduced (both effects can be achieved by increasing κ). In this paper we fix $\tau_m = m - \frac{1}{2}$ (i.e., $\delta = \frac{1}{2}$), which is valid for any $\eta < \frac{1}{2m}$; thereafter κ is chosen so that $w_\eta = \kappa^{-1} \log(\frac{1-\eta}{\eta})$ meets the desired geometric tolerance.

Theorem 5.7 (Single-layer MLP classifier on convex sets). *Let $C \subset \mathbb{R}^2$ be compact and convex and let $K \supset C$ be compact. For every $\varepsilon > 0$ there exist m, κ such that the decision set*

$$\Omega_{m,\kappa} := \{x \in K : F_{m,\kappa}(x) \geq \tau_m\}$$

satisfies $d_H(\Omega_{m,\kappa}, C) \leq \varepsilon$. Moreover, $F_{m,\kappa}$ is exactly of the finite-sum form (2.1) with weights $w_\ell = -\kappa u_\ell$, biases $\theta_\ell = \kappa h_\ell$, output weights $\alpha_\ell = 1$ ($\ell = 1, \dots, m$).

Proof. Pick C_{poly} as in (5.1) with $d_H(C_{\text{poly}}, C) \leq \varepsilon/2$. Fix $0 < \eta < \frac{1}{2}$. By Lemma 5.4, choose κ large so that the union of all uncertainty bands has Hausdorff thickness $< \varepsilon/2$. Then: (i) if x lies in the interior of C_{poly} , all m inequalities hold and $F_{m,\kappa}(x) \geq m(1 - \eta) > \tau_m$; (ii) if $x \notin C_{\text{poly}}$, at least one inequality fails and $F_{m,\kappa}(x) \leq (m - 1) + \eta < \tau_m$. Thus errors can only occur inside the thin bands, giving $d_H(\Omega_{m,\kappa}, C) \leq \varepsilon$. The finite-sum representation follows from (5.2). \square

Remark 5.8. The hard tropical classifier $\mathbf{1}\{F(x) \geq 0\}$ with the tropical polynomial $F = \bigoplus_\ell (h_\ell \odot \langle -u_\ell, x \rangle) = \max_\ell \{h_\ell - \langle u_\ell, x \rangle\}$ cuts out C_{poly} . Replacing the hard max by the soft transition gates (5.2) and counting satisfied constraints yields a smooth approximation of the same set. The tropical curve $\mathcal{T}(F)$ prescribes the piecewise-linear boundary and is dual to the subdivision of the Newton polygon $\delta(F)$.

Finite unions of convex sets

Let $C = \bigcup_{r=1}^R C_r$ with each $C_r \subset \mathbb{R}^2$ compact and convex. For component r , fix a supporting half-space description as in (5.1) with outward unit normals $\{u_{r,\ell}\}_{\ell=1}^{m_r}$ and support values $h_{r,\ell} \in \mathbb{R}$. Define the *half-space gates* (for a sharpness $\kappa > 0$)

$$s_{r,\ell}(x) := \sigma(\kappa(h_{r,\ell} - \langle u_{r,\ell}, x \rangle)), \quad \ell = 1, \dots, m_r, \quad r = 1, \dots, R. \quad (5.6)$$

Let $0 < \eta < \frac{1}{2}$ be fixed; by Lemma 5.4, each gate has an uncertainty band of thickness $\Theta(\kappa^{-1})$. For component r , define the *centered component score*

$$J_r(x) := \sum_{\ell=1}^{m_r} s_{r,\ell}(x) - \left(m_r - \frac{1}{2}\right). \quad (5.7)$$

Inside C_r , all constraints are satisfied so $J_r(x)$ is positive; outside C_r , at least one constraint is violated and $J_r(x)$ is negative.

Lemma 5.9. *Fix r and $0 < \eta < \frac{1}{2}$. There exists κ_0 such that for all $\kappa \geq \kappa_0$:*

(a) *If $x \in \text{int}(C_r)$ and $\text{dist}(x, \partial C_r) \geq t_\eta := \kappa^{-1} \log\left(\frac{1-\eta}{\eta}\right)$, then $s_{r,\ell}(x) \geq 1 - \eta$ for all ℓ and*

$$J_r(x) \geq m_r(1 - \eta) - \left(m_r - \frac{1}{2}\right) = \frac{1}{2} - m_r\eta.$$

(b) *If $x \notin C_r$ and $\text{dist}(x, \partial C_r) \geq t_\eta$, then at least one gate satisfies $s_{r,\ell^*}(x) \leq \eta$, while all others are ≤ 1 , hence*

$$J_r(x) \leq (m_r - 1) + \eta - \left(m_r - \frac{1}{2}\right) = -\frac{1}{2} + \eta.$$

Proof. By Lemma 5.4, if the signed distance to the supporting line $\langle u_{r,\ell}, x \rangle = h_{r,\ell}$ exceeds t_η on the *interior* side, then $s_{r,\ell}(x) \geq 1 - \eta$; if it exceeds t_η on the *exterior* side, then $s_{r,\ell}(x) \leq \eta$. Inside C_r , every inequality is satisfied, yielding (a). Outside C_r , at least one inequality is violated, yielding (b). \square

To construct an OR-like mechanism for the union of compact sets, we add a second layer. Pick a second sharpness $\lambda > 0$ and define

$$\Phi_{\kappa,\lambda}(x) := \sum_{r=1}^R \sigma(\lambda J_r(x)) = \sum_{r=1}^R \sigma\left(\lambda \left(\sum_{\ell=1}^{m_r} s_{r,\ell}(x) - \left(m_r - \frac{1}{2}\right)\right)\right). \quad (5.8)$$

Set the estimated classifier by thresholding this count at $\frac{1}{2}$:

$$\hat{\mathbf{1}}_C(x) = \mathbf{1}\{\Phi_{\kappa,\lambda}(x) \geq \frac{1}{2}\}. \quad (5.9)$$

Note that (i) the *first layer* consists of all gates $s_{r,\ell}$ in (5.6); (ii) the *second layer* forms J_r by the affine combination (5.7) and applies a sigmoid to each J_r ; (iii) the output is an affine sum (with weights 1) thresholded at $\frac{1}{2}$. Thus the whole construction is a two-layer sigmoidal MLP.

Theorem 5.10. *Let $C = \bigcup_{r=1}^R C_r \subset \mathbb{R}^2$ be a finite union of nonempty compact convex sets and let $K \supset C$ be compact. Fix $\varepsilon > 0$. For each r , choose outward unit normals $u_{r,\ell} \in \mathbb{S}^1$ and supports $h_{r,\ell} \in \mathbb{R}$, $\ell = 1, \dots, m_r$, so that*

$$C_r = \bigcap_{\ell=1}^{m_r} \{x : \langle u_{r,\ell}, x \rangle \leq h_{r,\ell}\}, \quad M := \max_{1 \leq r \leq R} m_r.$$

Let $\sigma(t) = \frac{1}{1+e^{-t}}$ be the logistic, strictly increasing with inverse $\sigma^{-1}(y) = \log\left(\frac{y}{1-y}\right)$. Fix any $0 < \eta < \min\{\frac{1}{2}, \frac{1}{4M}\}$ and define the η -strip half-width

$$t_\eta := \frac{1}{\kappa} \log\left(\frac{1-\eta}{\eta}\right) \quad (\kappa > 0 \text{ to be chosen}).$$

For each component r define the inner gates and the centered score

$$s_{r,\ell}(x) := \sigma(\kappa(h_{r,\ell} - \langle u_{r,\ell}, x \rangle)), \quad J_r(x) := \sum_{\ell=1}^{m_r} s_{r,\ell}(x) - \left(m_r - \frac{1}{2}\right),$$

and then the outer “OR-like” aggregator

$$\Phi_{\kappa,\lambda}(x) := \sum_{r=1}^R \sigma(\lambda J_r(x)) \quad (\lambda > 0).$$

Define the decision set

$$\Omega_{\kappa,\lambda} := \{x \in K : \Phi_{\kappa,\lambda}(x) \geq \frac{1}{2}\}.$$

Then there exist $\kappa, \lambda > 0$ such that $d_H(\Omega_{\kappa,\lambda}, C) \leq \varepsilon$. Moreover, for any $\delta \in (0, \frac{1}{2})$ set $a_\delta := \log(\frac{1-\delta}{\delta})$ and define

$$\mathcal{B}_{\text{in}} := \bigcup_{r,\ell} \left\{ x : |h_{r,\ell} - \langle u_{r,\ell}, x \rangle| \leq t_\eta \right\} \quad \text{and} \quad \mathcal{B}_{\text{out}} := \bigcup_{r=1}^R \left\{ x : |J_r(x)| \leq \frac{a_\delta}{\lambda} \right\}.$$

Outside the union of these two uncertainty bands,

$$x \notin \mathcal{B}_{\text{in}} \cup \mathcal{B}_{\text{out}} \implies \mathbf{1}\{\Phi_{\kappa,\lambda}(x) \geq \frac{1}{2}\} = 1_C(x).$$

In particular, if $\delta \in (0, \frac{1}{4R}]$, then the agreement holds uniformly on $K \setminus (\mathcal{B}_{\text{in}} \cup \mathcal{B}_{\text{out}})$, and the band thicknesses satisfy $\text{thick}(\mathcal{B}_{\text{in}}) = \Theta(\kappa^{-1})$ and $\text{thick}(\mathcal{B}_{\text{out}}) = \Theta(\lambda^{-1})$.

Proof. For a fixed gate $s_{r,\ell}(x) = \sigma(\kappa(h_{r,\ell} - \langle u_{r,\ell}, x \rangle))$ set the signed offset $d_{r,\ell}(x) := h_{r,\ell} - \langle u_{r,\ell}, x \rangle$. By monotonicity of σ and the explicit inverse $\sigma^{-1}(y)$, for any $\eta \in (0, \frac{1}{2})$:

$$s_{r,\ell}(x) \geq 1 - \eta \iff d_{r,\ell}(x) \geq \frac{1}{\kappa} \log\left(\frac{1-\eta}{\eta}\right) = t_\eta, \quad (5.10)$$

$$s_{r,\ell}(x) \leq \eta \iff d_{r,\ell}(x) \leq -t_\eta, \quad (5.11)$$

$$\eta \leq s_{r,\ell}(x) \leq 1 - \eta \iff |d_{r,\ell}(x)| \leq t_\eta. \quad (5.12)$$

Thus each inner gate transitions across a slab of geometric thickness $2t_\eta = \Theta(\kappa^{-1})$.

Step 1. Define the *interior* and *exterior* cores of C_r by

$$C_r^{\text{in}} := \{x \in C_r : \text{dist}(x, \partial C_r) \geq t_\eta\}, \quad C_r^{\text{ext}} := \{x \in K \setminus C_r : \text{dist}(x, \partial C_r) \geq t_\eta\}.$$

If $x \in C_r^{\text{in}}$, then all m_r inequalities are satisfied with margin at least t_η , hence by (5.10) we have $s_{r,\ell}(x) \geq 1 - \eta$ for every ℓ and

$$J_r(x) = \sum_{\ell=1}^{m_r} s_{r,\ell}(x) - \left(m_r - \frac{1}{2}\right) \geq m_r(1 - \eta) - \left(m_r - \frac{1}{2}\right) = \frac{1}{2} - m_r\eta \geq \frac{1}{2} - M\eta.$$

If $x \in C_r^{\text{out}}$, then at least one inequality is violated with exterior margin $\geq t_\eta$, so by (5.11) one gate is $\leq \eta$ while the rest are ≤ 1 ; hence

$$J_r(x) \leq (m_r - 1) + \eta - \left(m_r - \frac{1}{2}\right) = -\frac{1}{2} + \eta.$$

With the choice $\eta \leq \frac{1}{4M}$, these yield the uniform bounds

$$x \in C_r^{\text{in}} \Rightarrow J_r(x) \geq \frac{1}{4}, \quad x \in C_r^{\text{ext}} \Rightarrow J_r(x) \leq -\frac{1}{4}. \quad (5.13)$$

Step 2. Fix any $\delta \in (0, \frac{1}{4}]$ and set $a_\delta := \sigma^{-1}(1 - \delta) = \log(\frac{1-\delta}{\delta}) > 0$. Choose λ so that $\lambda \frac{1}{4} \geq a_\delta$, i.e.

$$\lambda \geq 4a_\delta. \quad (5.14)$$

Then $\sigma(\lambda t) \geq 1 - \delta$ for all $t \geq \frac{1}{4}$ and $\sigma(\lambda t) \leq \delta$ for all $t \leq -\frac{1}{4}$. Combining with (5.13) gives

$$x \in C_r^{\text{in}} \Rightarrow \sigma(\lambda J_r(x)) \geq 1 - \delta, \quad x \in C_r^{\text{out}} \Rightarrow \sigma(\lambda J_r(x)) \leq \delta. \quad (5.15)$$

Step 3. Let $C^{\text{in}} := \bigcup_{r=1}^R C_r^{\text{in}}$ and $C^{\text{ext}} := \bigcap_{r=1}^R C_r^{\text{ext}}$. If $x \in C^{\text{in}}$, pick r^* with $x \in C_{r^*}^{\text{in}}$. Then, by (5.15),

$$\Phi_{\kappa,\lambda}(x) = \sum_{r=1}^R \sigma(\lambda J_r(x)) \geq \sigma(\lambda J_{r^*}(x)) \geq 1 - \delta > \frac{1}{2},$$

so $x \in \Omega_{\kappa,\lambda}$. Conversely, if $x \in C^{\text{out}}$, then (5.15) gives $\Phi_{\kappa,\lambda}(x) \leq R\delta$. Taking $\delta \leq \frac{1}{4R}$ ensures $\Phi_{\kappa,\lambda}(x) < \frac{1}{2}$, hence $x \notin \Omega_{\kappa,\lambda}$.

Step 4. Misclassifications can only occur where the implications used above are not guaranteed, namely within the union of:

- (i) inner bands $B_{\kappa} := \bigcup_{r,\ell} \left\{ x : |h_{r,\ell} - \langle u_{r,\ell}, x \rangle| \leq t_{\eta} \right\}$, thickness $2t_{\eta} = \frac{2}{\kappa} \log\left(\frac{1-\eta}{\eta}\right) = \Theta(\kappa^{-1})$;
- (ii) outer bands $Z_{\lambda,\delta} := \bigcup_r \left\{ x : |J_r(x)| \leq \frac{a_{\delta}}{\lambda} \right\}$, since $|J_r| > \frac{a_{\delta}}{\lambda} \Rightarrow \sigma(\lambda J_r) \in \{\leq \delta, \geq 1 - \delta\}$.

The “transition window” in the *argument* of the outer sigmoid is exactly $[-\frac{a_{\delta}}{\lambda}, \frac{a_{\delta}}{\lambda}]$, so the effective geometric thickness of $Z_{\lambda,\delta}$ scales as $\Theta(\lambda^{-1})$.

Step 5. Since K is compact, we may choose κ, λ large enough so that the Minkowski (thickness) of $B_{\kappa} \cup Z_{\lambda,\delta}$ is $< \varepsilon$. Then:

$$C \subseteq \mathcal{N}_{\varepsilon}(\Omega_{\kappa,\lambda}) \quad \text{and} \quad \Omega_{\kappa,\lambda} \subseteq \mathcal{N}_{\varepsilon}(C),$$

which is equivalent to $d_H(\Omega_{\kappa,\lambda}, C) \leq \varepsilon$.

For $x \notin B_{\kappa}$, each inner gate is saturated: $s_{r,\ell}(x) \in [0, \eta] \cup [1 - \eta, 1]$. Hence, for any component r ,

$$\begin{aligned} x \in C_r &\Rightarrow J_r(x) = \sum_{\ell=1}^{m_r} s_{r,\ell}(x) - \left(m_r - \frac{1}{2}\right) \geq m_r(1 - \eta) - \left(m_r - \frac{1}{2}\right) = \frac{1}{2} - m_r\eta, \\ x \notin C_r &\Rightarrow J_r(x) \leq (m_r - 1) \cdot 1 + \eta - \left(m_r - \frac{1}{2}\right) = \eta - \frac{1}{2}. \end{aligned}$$

With $\eta < \min\{\frac{1}{2}, \frac{1}{4M}\}$ we get the uniform margin $J_r(x) \geq \frac{1}{4}$ if $x \in C_r$ and $J_r(x) \leq -\frac{1}{4}$ if $x \notin C_r$. Now, for $x \notin Z_{\lambda,\delta}$ we also have outer saturation: $s_r(x) = \sigma(\lambda J_r(x)) \in [0, \delta] \cup [1 - \delta, 1]$ with the same split as above. Therefore:

$$x \notin C \Rightarrow \Phi(x) = \sum_{r=1}^R s_r(x) \leq R\delta, \quad x \in C \Rightarrow \Phi(x) \geq 1 - \delta.$$

Choosing $\delta \leq \frac{1}{4R}$ yields $\Phi(x) \leq \frac{1}{4} < \frac{1}{2}$ for $x \notin C$ and $\Phi(x) \geq 1 - \delta \geq \frac{3}{4} > \frac{1}{2}$ for $x \in C$. Hence the final constructed classifier agrees with 1_C pointwise on $K \setminus (B_{\kappa} \cup Z_{\lambda,\delta})$, i.e., $\mathbf{1}\{\Phi(x) \geq \frac{1}{2}\} = 1_C(x)$ holds pointwise on $K \setminus (B_{\kappa} \cup Z_{\lambda,\delta})$. \square

Remark 5.11. The construction realizes a two-layer sigmoidal MLP in the classical finite-sum format. Layer 1 (all inner gates): weights $w_{r,\ell} = -\kappa u_{r,\ell}$, biases $\theta_{r,\ell} = \kappa h_{r,\ell}$, unit outgoing weights. Layer 2 (per-component centering and squash): for component r , form $J_r = \sum_{\ell=1}^{m_r} s_{r,\ell} - (m_r - \frac{1}{2})$ and apply $\sigma(\cdot)$. Output layer: unit weights summing the R outer activations and threshold at 1/2.

Algorithm 2 Geometry-aware MLP initializer for $\mathbb{R}^2 \rightarrow \{0, 1\}$

Input: Target set: either (i) a convex polygon C with CCW vertices (v_1, \dots, v_m) , or (ii) a finite union $\bigcup_{r=1}^R C_r$ of such polygons with CCW vertices; gate sharpness $\kappa > 0$; (optional) second sharpness $\lambda > 0$

- 1: **for** each component C_r with CCW vertices $(v_{r,1}, \dots, v_{r,m_r})$ **do**
- 2: **for** $i = 1$ to m_r **do**
- 3: Let $e_{r,i} \leftarrow v_{r,i+1} - v_{r,i}$ with $v_{r,m_r+1} \equiv v_{r,1}$
- 4: set $u_{r,i} \leftarrow \frac{(e_{r,i})^{\perp_R}}{\|e_{r,i}\|}$ where $(a, b)^{\perp_R} := (b, -a)$ ▷ CCW vertices \Rightarrow right-normal is outward
- 5: **(Support value)** $h_{r,i} \leftarrow \langle u_{r,i}, v_{r,i} \rangle$
- 6: **(Inner gate / facet classifier)** $s_{r,i}(x) \leftarrow \sigma(\kappa [h_{r,i} - \langle u_{r,i}, x \rangle])$
- 7: **end for**
- 8: **(Per-component score)** $J_r(x) \leftarrow \sum_{i=1}^{m_r} s_{r,i}(x) - (m_r - \frac{1}{2})$
- 9: **(Per-component decision gate)** $s_r(x) \leftarrow \sigma(\lambda J_r(x))$
- 10: **end for**
- 11: **if** $R = 1$ (single component) **then**
- 12: **Classifier:** $\hat{y}(x) \leftarrow \mathbf{1}\{J_1(x) \geq 0\}$
- 13: **else**
- 14: **OR-like aggregator:** $\Phi_{\kappa,\lambda}(x) \leftarrow \sum_{r=1}^R s_r(x)$
- 15: **Classifier:** $\hat{y}(x) \leftarrow \mathbf{1}\{\Phi_{\kappa,\lambda}(x) \geq \frac{1}{2}\}$
- 16: **end if**
- 17: For each facet gate $s_{r,i}(x) = \sigma(\langle w_{r,i}, x \rangle + \theta_{r,i})$, set

$$w_{r,i} = -\kappa u_{r,i}, \quad \theta_{r,i} = \kappa h_{r,i}, \quad \alpha_{r,i} \equiv 1.$$

- 18: **Return** $\{(w_{r,i}, \theta_{r,i}, \alpha_{r,i})\}$ for all (r, i) , together with (λ) if using the outer gates.

Complexity and accuracy. If ∂C is C^2 with bounded curvature, circumscribed m -gons achieve $\mathcal{O}(m^{-2})$ Hausdorff error; the sigmoid band adds $\mathcal{O}(\kappa^{-1})$ thickness. Taking $m = \Theta(\varepsilon^{-1/2})$ and $\kappa = \Theta(\varepsilon^{-1})$ yields overall error $\mathcal{O}(\varepsilon)$. Network size is $N = \Theta(m)$ for a single component and $N = \Theta(\sum_r m_r)$ for unions.

Remark 5.12 (Why $\tau = \frac{1}{2} \min_r m_r$?). Each component C_r has m_r gates. Deep inside C_r , all its gates contribute ≈ 1 , so the component's sum is $\approx m_r$. Outside C_r , at least one gate contributes ≈ 0 , so the component's sum is $\lesssim m_r - 1$. We do not know *which* component contains a given interior point of the union; therefore we pick a single threshold that any interior point can pass using only the *smallest* component. Setting

$$\tau = \frac{1}{2} \min_r m_r$$

guarantees: (i) if $x \in C_r$ and is away from ∂C_r , then the single component C_r already yields $\sum_{\ell=1}^{m_r} s_{r,\ell}(x) \geq 2\tau$, so x is accepted; (ii) if $x \notin \bigcup_r C_r$, then every component is missing at least one satisfied facet and the total score stays below τ once the gates are steep (large κ), hence x is rejected. Thus $\tau = \frac{1}{2} \min_r m_r$ is a conservative, component-agnostic threshold that makes a single “active” piece sufficient for acceptance while preventing spurious acceptance outside the union.

Remark 5.13 (Tropical summary). The parameters $\{(u_\ell, h_\ell)\}$ induces a tropical polynomial $F(x) = \bigoplus_\ell (h_\ell \odot \langle -u_\ell, x \rangle)$ with curve $\mathcal{T}(F)$ dual to $\delta(F)$. Our initializer replaces the hard set $\{F \geq 0\}$ by soft gates (5.2) and implements the decision $\mathbf{1}\{F_{m,\kappa} \geq \tau_m\}$. Thus the learned

boundary starts aligned with $\mathcal{T}(F)$ (up to a band of width $\Theta(\kappa^{-1})$) and can be refined by standard training without leaving the finite-sum form in (2.1).

6 General Planar Regions

Section 5 constructed a two-layer sigmoidal MLP for convex targets and for finite unions of convex sets. We now extend the construction to *arbitrary nonconvex* planar targets by reducing them to finite unions of disks. The only assumption is compactness, which gives both existence of finite subcovers and Hausdorff-metric control.

Finite ball covers from Heine–Borel. Let $C \subset \mathbb{R}^2$ be nonempty and compact. By Heine–Borel, every open cover of C admits a finite subcover. In particular, for any $\varepsilon > 0$ there exist centers and radii $\{(c_j, r_j)\}_{j=1}^{R_B}$ such that

$$C \subseteq \bigcup_{j=1}^{R_B} \overline{B}(c_j, r_j) \subseteq \mathcal{N}_\varepsilon(C),$$

so the finite union of *closed* disks ε -covers C in the Hausdorff sense. This reduces the general (possibly highly nonconvex) C to a finite union of convex pieces.

For each disk $\overline{B}(c_j, r_j)$ choose a circumscribed regular m_j -gon

$$P_j = \bigcap_{\ell=1}^{m_j} \{x : \langle u_{j,\ell}, x \rangle \leq h_{j,\ell}\}, \quad u_{j,\ell} = (\cos \frac{2\pi\ell}{m_j}, \sin \frac{2\pi\ell}{m_j}), \quad h_{j,\ell} = \langle u_{j,\ell}, c_j \rangle + r_j,$$

so that $d_H(P_j, \overline{B}(c_j, r_j)) = \mathcal{O}(r_j m_j^{-2})$. Now apply §5 paradigm: attach to each half-space a sharp sigmoid gate $s_{j,\ell}(x) = \sigma(\kappa[h_{j,\ell} - \langle u_{j,\ell}, x \rangle])$, center the per-polygon sum $J_j(x) = \sum_{\ell=1}^{m_j} s_{j,\ell}(x) - (m_j - \frac{1}{2})$, squash J_j once more $s_j^{\text{out}}(x) = \sigma(\lambda J_j(x))$, and aggregate with a OR-like mechanism $\Phi_{\kappa,\lambda}(x) = \sum_{j=1}^{R_B} s_j^{\text{out}}(x)$, classifying by $\widehat{\mathbf{1}}_C(x) = \mathbf{1}\{\Phi_{\kappa,\lambda}(x) \geq \frac{1}{2}\}$. This is exactly the two-layer sigmoidal MLP architecture already established for finite unions of convex sets (see 5.10).

Theorem 6.1. *Let $C \subset \mathbb{R}^2$ be nonempty and compact. For every $\varepsilon > 0$ there exist a finite ball cover $\{\overline{B}(c_j, r_j)\}_{j=1}^{R_B}$, polygon side counts $\{m_j\}$, and slopes $\kappa, \lambda > 0$ such that the decision set $\widehat{C} := \{x : \widehat{\mathbf{1}}_C(x) = 1\}$ produced by the above MLP satisfies*

$$d_H(\widehat{C}, C) \leq \varepsilon.$$

Moreover, away from two thin “uncertainty bands”—the inner facet bands of thickness $\mathcal{O}(\kappa^{-1})$ and the outer per-ball bands of thickness $\mathcal{O}(\lambda^{-1})$ —the classifier agrees pointwise with $\mathbf{1}_C$ (same margins as discussed in 5.10).

Proof. Fix $\varepsilon > 0$,

(i) *Finite cover (Heine–Borel).* Since C is compact, by Heine–Borel there exists a finite family of closed disks $\{\overline{B}(c_j, r_j)\}_{j=1}^{R_B}$ with $C \subseteq \bigcup_j \overline{B}(c_j, r_j) \subseteq \mathcal{N}_{\varepsilon_{\text{cov}}}(C)$.

(ii) *Disk \rightarrow polygon.* For each j , let P_j be a circumscribed regular m_j -gon: $P_j = \bigcap_{\ell=1}^{m_j} \{x : \langle u_{j,\ell}, x \rangle \leq h_{j,\ell}\}$, with $u_{j,\ell} = (\cos \frac{2\pi\ell}{m_j}, \sin \frac{2\pi\ell}{m_j})$ and $h_{j,\ell} = \langle u_{j,\ell}, c_j \rangle + r_j$. Choose m_j large enough so that $d_H(P_j, \overline{B}(c_j, r_j)) \leq \varepsilon_{\text{poly}}$ for all j (e.g. using the bound $r_j(1 - \cos(\pi/m_j)) = \mathcal{O}(r_j m_j^{-2})$). Then $\bigcup_j P_j \subseteq \bigcup_j \overline{B}(c_j, r_j) \subseteq \mathcal{N}_{\varepsilon_{\text{cov}}}(C)$ and $\bigcup_j \overline{B}(c_j, r_j) \subseteq \mathcal{N}_{\varepsilon_{\text{poly}}}(\bigcup_j P_j)$. Thus $d_H(\bigcup_j P_j, C) \leq \varepsilon_{\text{cov}} + \varepsilon_{\text{poly}}$.

(iii) *Compile $\bigcup_j P_j$ by Theorem 5.10.* Apply the union-of-convexes construction (Section 5) to the family $\{P_j\}$. By Theorem 5.10, there exist slopes $\kappa, \lambda > 0$ such that: (a) outside the inner facet bands of half-width $t_{\text{in}} = \kappa^{-1} \log(\frac{1-\eta}{\eta})$ and the outer per-ball bands of half-width

$t_{\text{out}} = \lambda^{-1} \log(\frac{1-\delta}{\delta})$, the classifier agrees pointwise with $1_{\bigcup_j P_j}$ with fixed positive margins; and (b) the geometric thickness of these bands scales as $\mathcal{O}(\kappa^{-1})$ and $\mathcal{O}(\lambda^{-1})$, respectively. Choose κ, λ so that the total thickness of the inner bands is $\leq \varepsilon_{\text{in}}$ and that of the outer bands is $\leq \varepsilon_{\text{out}}$, which is possible by taking κ, λ sufficiently large.

(iv) *Hausdorff*. Let \widehat{C} be the decision set. From (iii) we have $d_H(\widehat{C}, \bigcup_j P_j) \leq \varepsilon_{\text{in}} + \varepsilon_{\text{out}}$. Combining with (ii) gives

$$d_H(\widehat{C}, C) \leq d_H(\widehat{C}, \bigcup_j P_j) + d_H(\bigcup_j P_j, C) \leq (\varepsilon_{\text{in}} + \varepsilon_{\text{out}}) + (\varepsilon_{\text{cov}} + \varepsilon_{\text{poly}}) =: \varepsilon.$$

Finally, the pointwise agreement away from the two bands and the margin values are exactly those stated in Theorem 5.10, applied componentwise to $\{P_j\}$. \square

The Nerve Theorem. Although the network construction above is entirely analytic, the same ball cover also yields a concise *topological* summary. Inflate each disk to an open set $U_j := B(c_j, r_j + \rho)$ for small $\rho > 0$. Then $\mathcal{U} = \{U_j\}$ is a good open cover (all finite intersections are convex, hence contractible), so the Nerve Theorem gives a homotopy equivalence

$$\text{Nerve}(\mathcal{U}) \simeq \bigcup_{j=1}^{R_B} U_j \quad [6, 12].$$

Under mild geometric conditions (e.g., C has positive reach), sufficiently small offsets $\mathcal{N}_\rho(C)$ deformation-retract onto C , whence for small enough ρ also $\text{Nerve}(\mathcal{U}) \simeq C$ [27]. This mirrors the logic in manifold learning (e.g., UMAP), where good covers and Čech nerves certify that the simplicial model captures the correct homotopy type at an appropriate scale [22]. In short, *the cover that drives our MLP approximation simultaneously provides a simplicial certificate of the target's topology*—with no changes to the network.

Algorithm 3 Ball cover \Rightarrow two-layer sigmoidal MLP

Input: Compact window $K \supset C$; tolerance split $(\varepsilon_{\text{cov}}, \varepsilon_{\text{poly}})$; sharpness (κ, λ) or margin targets (η, δ) with $\eta < \frac{1}{4M}$ ($M := \max_j m_j$) and $\delta \leq \frac{1}{4R_B}$

Output: A two-layer sigmoidal MLP with decision set \widehat{C} and $d_H(\widehat{C}, C) \lesssim \varepsilon_{\text{cov}} + \varepsilon_{\text{poly}} + \mathcal{O}(\kappa^{-1}) + \mathcal{O}(\lambda^{-1})$

- 1: **Finite ball cover:** Choose $\{\overline{B}(c_j, r_j)\}_{j=1}^{R_B}$ such that $C \subseteq \bigcup_j \overline{B}(c_j, r_j) \subseteq \mathcal{N}_{\varepsilon_{\text{cov}}}(C)$.
- 2: **Polygonize each ball:** For disk j , pick m_j and angles $\theta_{j,\ell} = 2\pi\ell/m_j$; set $u_{j,\ell} = (\cos \theta_{j,\ell}, \sin \theta_{j,\ell})$ and $h_{j,\ell} = \langle u_{j,\ell}, c_j \rangle + r_j$. Then $P_j = \bigcap_\ell \{x : \langle u_{j,\ell}, x \rangle \leq h_{j,\ell}\}$ with $d_H(P_j, \overline{B}(c_j, r_j)) = \mathcal{O}(r_j m_j^{-2})$.
- 3: **Inner gates:** $s_{j,\ell}(x) = \sigma(\kappa [h_{j,\ell} - \langle u_{j,\ell}, x \rangle])$, $J_j(x) = \sum_{\ell=1}^{m_j} s_{j,\ell}(x) - (m_j - \frac{1}{2})$.
- 4: **Outer gates (OR-like aggregator):** $s_j^{\text{out}}(x) = \sigma(\lambda J_j(x))$, $\Phi(x) = \sum_{j=1}^{R_B} s_j^{\text{out}}(x)$, $\widehat{1}_C(x) = \mathbf{1}\{\Phi(x) \geq \frac{1}{2}\}$.
- 5: **Weights:** Inner: $w_{j,\ell} = -\kappa u_{j,\ell}$, $\theta_{j,\ell} = \kappa h_{j,\ell}$, output weight = 1. Outer (per ball): affine map J_j followed by $\sigma(\lambda \cdot)$; final layer sums with unit weights.

Complexity Fix $\varepsilon > 0$ and split the budget as $\varepsilon_{\text{cov}} + \varepsilon_{\text{poly}} + c_1 \kappa^{-1} + c_2 \lambda^{-1} \leq \varepsilon$, with $c_1 = \log \frac{1-\eta}{\eta}$ and $c_2 = \log \frac{1-\delta}{\delta}$ (inner/outer margins; $\eta < \frac{1}{4M}$, $M := \max_j m_j$, $\delta \leq \frac{1}{4R_B}$). For disk j (radius r_j), choose $m_j = \Theta(\sqrt{r_j/\varepsilon_{\text{poly}}})$ so $d_H(P_j, \overline{B}) = \mathcal{O}(r_j m_j^{-2}) \leq \varepsilon_{\text{poly}}$, hence the total inner units are $N_{\text{inner}} = \sum_j m_j = \Theta(\sum_j \sqrt{r_j/\varepsilon_{\text{poly}}})$ and the outer units equal R_B ; parameters and per-point cost are $\Theta(N_{\text{inner}})$ (since $m_j \gg 1$). The Hausdorff error obeys $d_H(\widehat{C}, C) \leq \varepsilon_{\text{cov}} + \varepsilon_{\text{poly}} + c_1 \kappa^{-1} + c_2 \lambda^{-1}$.

7 Beyond the Plane: Higher-Dimensional Extensions

This section extends the constructions of §5–6 from the plane to \mathbb{R}^d ($d \geq 2$) without changing the network architecture in the form (2.1). The pointwise guarantees, Hausdorff control, and complexity decomposition remain the same; only the construction of covers is replaced by ball→polytope with the standard high-dimensional approximation rate.

Ball → polytope in \mathbb{R}^d . Let $\overline{B}(c, r) \subset \mathbb{R}^d$ be a closed Euclidean ball. An m -facet circumscribed polytope P satisfies

$$d_H(P, \overline{B}(c, r)) = \mathcal{O}(r m^{-2/(d-1)}).$$

Hence choosing

$$m_j = \Theta\left(\left(\frac{r_j}{\varepsilon_{\text{poly}}}\right)^{\frac{d-1}{2}}\right) \Rightarrow d_H(P_j, \overline{B}(c_j, r_j)) \leq \varepsilon_{\text{poly}}.$$

Theorem 7.1 (Union of convex sets in \mathbb{R}^d (high-dimensional version of Thm.5.10)). *Let $C = \bigcup_{r=1}^R C_r \subset \mathbb{R}^d$ be a finite union of nonempty compact convex sets and let $K \supset C$ be compact. For component r , fix outward unit normals $u_{r,\ell} \in \mathbb{S}^{d-1}$ and supports $h_{r,\ell} \in \mathbb{R}$ ($\ell = 1, \dots, m_r$), and define inner gates and centered score*

$$s_{r,\ell}(x) := \sigma(\kappa [h_{r,\ell} - \langle u_{r,\ell}, x \rangle]), \quad J_r(x) := \sum_{\ell=1}^{m_r} s_{r,\ell}(x) - \left(m_r - \frac{1}{2}\right).$$

Let the “OR-like” aggregator be

$$\Phi_{\kappa,\lambda}(x) := \sum_{r=1}^R \sigma(\lambda J_r(x)), \quad \widehat{\mathbf{1}}_C(x) := \mathbf{1}\{\Phi_{\kappa,\lambda}(x) \geq \frac{1}{2}\}.$$

Fix $0 < \eta < \min\{\frac{1}{2}, \frac{1}{4M}\}$ with $M := \max_r m_r$, and $0 < \delta \leq \frac{1}{4R}$, and set

$$c_1 := \log \frac{1-\eta}{\eta}, \quad c_2 := \log \frac{1-\delta}{\delta}.$$

Then there exist $\kappa, \lambda > 0$ such that, outside the two uncertainty bands

$$\mathcal{B}_{\text{in}} := \bigcup_{r,\ell} \left\{ x : |h_{r,\ell} - \langle u_{r,\ell}, x \rangle| \leq \frac{c_1}{\kappa} \right\}, \quad \mathcal{B}_{\text{out}} := \bigcup_{r=1}^R \left\{ x : |J_r(x)| \leq \frac{c_2}{\lambda} \right\},$$

we have $\mathbf{1}\{\Phi_{\kappa,\lambda}(x) \geq \frac{1}{2}\} = \mathbf{1}_C(x)$. Moreover,

$$\text{thick}(\mathcal{B}_{\text{in}}) = \Theta(\kappa^{-1}), \quad \text{thick}(\mathcal{B}_{\text{out}}) = \Theta(\lambda^{-1}).$$

Proof. The proof is similar to the planar case: Lemma 5.4 is dimension-free, so the inner/outer margin arguments and the saturation outside bands carry over verbatim. \square

Theorem 7.2 (Compact sets via ball covers in \mathbb{R}^d (high-dimensional version of Thm.6.1)). *Let $C \subset \mathbb{R}^d$ be nonempty and compact. For every $\varepsilon > 0$ there exist a finite ball cover $\{\overline{B}(c_j, r_j)\}_{j=1}^{R_B}$, per-ball facet counts $m_j = \Theta((r_j/\varepsilon_{\text{poly}})^{(d-1)/2})$, and slopes $\kappa, \lambda > 0$ such that the two-layer sigmoidal MLP classifier built exactly as in §6 produces a decision set \widehat{C} with*

$$d_H(\widehat{C}, C) \leq \varepsilon_{\text{cov}} + \varepsilon_{\text{poly}} + c_1 \kappa^{-1} + c_2 \lambda^{-1} \leq \varepsilon,$$

and, away from the inner/outer bands of thicknesses $\Theta(\kappa^{-1})$ and $\Theta(\lambda^{-1})$, agrees pointwise with $\mathbf{1}_C$.

Proof. This theorem is a trivial result of Heine–Borel (finite cover), ball→polytope with m_j as above, and Theorem 7.1. Details are similar to Thm. 6.1 \square

Complexity. Let $\varepsilon > 0$ and split the budget

$$\varepsilon_{\text{tot}} := \varepsilon_{\text{cov}} + \varepsilon_{\text{poly}} + c_1 \kappa^{-1} + c_2 \lambda^{-1} \leq \varepsilon, \quad c_1 = \log \frac{1-\eta}{\eta}, \quad c_2 = \log \frac{1-\delta}{\delta}.$$

For ball j of radius r_j ,

$$m_j = \Theta\left(\left(\frac{r_j}{\varepsilon_{\text{poly}}}\right)^{\frac{d-1}{2}}\right), \quad N_{\text{inner}} = \sum_{j=1}^{R_B} m_j, \quad N_{\text{outer}} = R_B, \quad \text{cost} = \Theta(N_{\text{inner}}).$$

Remark 7.3 (Tropical viewpoint in higher d). Let

$$F(x) = \bigoplus_{\ell=1}^m (h_\ell \odot x^{-u_\ell}) = \max_{1 \leq \ell \leq m} \{ h_\ell - \langle u_\ell, x \rangle \}, \quad u_\ell \in \mathbb{S}^{d-1}.$$

The hard classifier on a convex component is the tropical inequality

$$\mathbf{1}\{F(x) \geq 0\} = \mathbf{1}\left\{ \bigoplus_{\ell} (h_\ell \odot x^{-u_\ell}) \geq 0 \right\},$$

i.e., membership in the intersection of supporting tropical half-spaces. Our sigmoidal MLP replaces each hard tropical term $h_\ell \odot x^{-u_\ell}$ by a steep gate $s_\ell(x) = \sigma(\kappa[h_\ell - \langle u_\ell, x \rangle])$ and aggregates by (soft) counting satisfied constraints in place of the hard tropical sum \oplus . The tropical hypersurface $\mathcal{T}(F)$ is dual to the induced subdivision of the Newton polytope $\delta(F)$; this duality (orthogonality, adjacency, and dimension reversal) carries over verbatim in \mathbb{R}^d .

8 Numerical Studies

We do the numerical studies on the proposed geometry-aware construction with three different planar regions: (i) a *single disk*, (ii) a *two-disk union*, and (iii) a *nonconvex swiss-roll* set approximated by a union of ε -balls. All models are purely sigmoidal MLP form as in (2.1) trained with *binary cross-entropy* (BCE) using the *Adam* optimizer [19]. We report the *Brier score* [4], the area under curve (*AUC*; [11]), and the *intersection-over-union* at threshold 0.5 (*IoU*; [18]).

Experiment Setup. For the **single** and **two-disk** tasks we draw inputs uniformly from the window $K = [-2, 2]^2 \subset \mathbb{R}^2$; the training and evaluation set sizes are **TRAIN_N** = 12,000 and **TEST_N** = 3,000. Both disks have radius $R = 0.8$ with centers $C_1 = (-0.6, 0.0)$ and $C_2 = (0.6, 0.0)$. We test hidden sizes $H \in \{16, 32\}$ and compare the five initializations. Training uses 80 epochs, batch size 512, Adam with learning rate 3×10^{-3} .

In the geometry-aware construction (Secs. 5–6), each inner half-space gate takes the form

$$s_\ell(x) = \sigma(\kappa [h_\ell - \langle u_\ell, x \rangle]),$$

with logistic sigmoid $\sigma(\cdot)$ and sharpness $\kappa = \kappa_{\text{hidden}} = 30.0$. Evaluation uses a 200×200 grid over K and a threshold $\tau = 0.5$.

Initialization methods. We compare our construction with four classic initialization schemes; throughout, training follows the exact protocol above, and no data-dependent pretraining is used.

1. **Random** — Draw weights from *uniform* distributions. [9, 13]
2. **Xavier** — Initialize fully connected layers with Xavier-uniform to stabilize signal and gradients in sigmoidal multilayer perceptrons. [9]

3. **Kaiming (uniform)** — Use Kaiming–uniform for hidden layers and linear-consistent scaling for heads; serves as a rectifier-scaled baseline in our smooth setting. [13]
4. **He (normal)** — Sample hidden weights with He–normal (Gaussian) and keep linear-consistent heads. [13, 23]

8.1 Non-convex example : Swiss-roll

Following Sec. 6, we approximate the nonconvex swiss–roll target by a finite union of ε –balls on the plane, where $\varepsilon = 1.5$. Positives are identified on a uniform window and treated as candidate centers. We then (i) *Voxel downsampling*. Let $v := \varepsilon \times \text{VOXEL_RATIO} = 1.5 \times 0.6$. We quantize each candidate point $p \in \mathbb{R}^2$ to a grid cell by $q = \lfloor p/v \rfloor$ and retain a single representative per occupied cell (e.g., the first point). This “one-per-voxel” rule removes near-duplicate centers within distance $\lesssim v$, yielding a thinner, spatially uniform candidate set for next step. (ii) apply *Farthest Point Sampling* (FPS)—the classical greedy k –center algorithm [10]—to select at most $\text{FPS_BUDGET} = 120$ centers. The resulting cover drives the constructive initializer: for each selected center we place $H_{\text{sides}} = 24$ steep half–planes (inner sharpness $\kappa_{\text{hidden}} = 8.0$, per–disk sharpness $\kappa_{\text{disk}} = 6.0$), and use an OR–like head $\alpha(\sum_k s_k - \tau)$ with $\alpha = 6.0$ and $\tau = 0.5$. This is the example construction of the two–layer sigmoidal construction from Sec. 6 within the form (2.1).

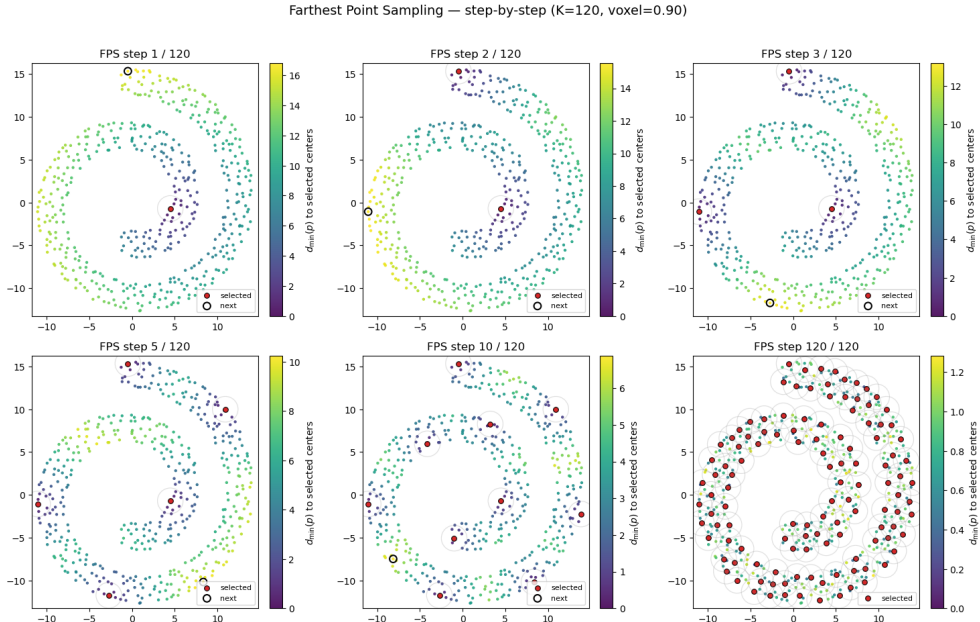


Figure 4: How Farthest Point Sampling choose centers

Metrics. Let $\{(x_i, y_i)\}_{i=1}^N$ be a binary dataset with $y_i \in \{0, 1\}$. The model outputs a logit $z_i \in \mathbb{R}$ and a probability $p_i := \sigma(z_i) \in [0, 1]$, where $\sigma(t) = (1 + e^{-t})^{-1}$. Write $P := \{i : y_i = 1\}$ and $N := \{i : y_i = 0\}$.

(i) *Brier score*.[4] The mean squared error between calibrated probabilities and labels:

$$\text{Brier} := \frac{1}{N} \sum_{i=1}^N (p_i - y_i)^2.$$

(ii) *Area under the ROC curve (AUC)*.[11] Using scores p_i (higher means more positive), the

empirical AUC is the Wilcoxon–Mann–Whitney statistic:

$$\text{AUC} := \frac{1}{|P||N|} \sum_{i \in P} \sum_{j \in N} \left[\mathbf{1}\{p_i > p_j\} + \frac{1}{2} \mathbf{1}\{p_i = p_j\} \right],$$

(iii) *Intersection-over-Union at threshold τ (IoU@ τ).* [18] Let $\hat{y}_i(\tau) := \mathbf{1}\{p_i \geq \tau\}$ be the predicted label at threshold τ (we use $\tau = 0.5$ in this section). Then

$$\text{IoU}(\tau) := \frac{\sum_{i=1}^N \mathbf{1}\{\hat{y}_i(\tau) = 1, y_i = 1\}}{\sum_{i=1}^N \mathbf{1}\{\hat{y}_i(\tau) = 1 \text{ or } y_i = 1\}}$$

8.2 Quantitative results

Table 1 summarizes single- and two-disk results under the exact protocol above. The geometry-aware initializer provides a near-perfect boundary at *initialization* for the single-disk case (AUC = 1.0000, IoU ≥ 0.9814) and markedly stronger IoU for the two-disk union (AUC ≥ 0.9890 , IoU ≥ 0.7395) compared to geometry-agnostic baselines. After training, all methods reach near-perfect AUC and high IoU; nonetheless, our construction is the only one that starts with a closed boundary on the tasks, reducing the reliance on optimization to *refine* rather than *discover* geometry.

Case	H	Init	Init Brier	Init AUC	Init IoU	Final Brier	Final AUC	Final IoU
Single	16	random	0.4176	0.4861	0.1255	0.0089	0.9999	0.9548
		xavier	0.2086	0.4965	0.0805	0.0056	1.0000	0.9767
		kaiming	0.3943	0.5154	0.1336	0.0073	1.0000	0.9727
		he	0.1441	0.5194	0.0000	0.0045	1.0000	0.9794
	16	ours	0.0216	1.0000	0.9954	0.0066	0.9999	0.9634
	32	random	0.1263	0.5119	0.0000	0.0034	1.0000	0.9828
		xavier	0.3518	0.5197	0.1295	0.0049	1.0000	0.9760
		kaiming	0.2322	0.5034	0.1050	0.0038	1.0000	0.9874
		he	0.1875	0.5116	0.0000	0.0038	1.0000	0.9807
	32	ours	0.0193	1.0000	0.9814	0.0026	1.0000	0.9874
Double	16	random	0.2365	0.5038	0.1626	0.0057	0.9996	0.9709
		xavier	0.3645	0.5047	0.2297	0.0081	0.9995	0.9573
		kaiming	0.4116	0.4951	0.1771	0.0070	0.9996	0.9611
		he	0.2374	0.5098	0.1626	0.0045	0.9998	0.9795
	16	ours	0.0659	0.9890	0.7395	0.0102	0.9993	0.9496
	32	random	0.2538	0.5003	0.1972	0.0033	1.0000	0.9870
		xavier	0.3771	0.5001	0.1867	0.0055	0.9998	0.9719
		kaiming	0.2227	0.4902	0.0000	0.0031	0.9999	0.9870
		he	0.2235	0.4963	0.0806	0.0043	0.9999	0.9774
	32	ours	0.0601	0.9934	0.7757	0.0066	0.9999	0.9751

Table 1: Results of single and two-disk tasks: Brier, AUC, and IoU@0.5 at initialization and after training (single/two-disk: epochs = 80, batch = 512, learning rate = 3×10^{-3}). Best initialization per block in **bold**.

On the **single-disk** task, our initializer achieves near-perfect geometry at initialization (AUC = 1.0000, IoU > 0.98). After training, all methods converge to near-perfect AUCs. On the **two-disk union**, our OR-like aggregator produces a faithful union boundary already at initialization, reflected in high IoU; subsequent training mainly refines calibration.

8.3 Qualitative results

We visualize (i) the data distributions (positives / negatives), (ii) decision maps at initialization and after training for $H = 32$, and (iii) loss curves for each H .

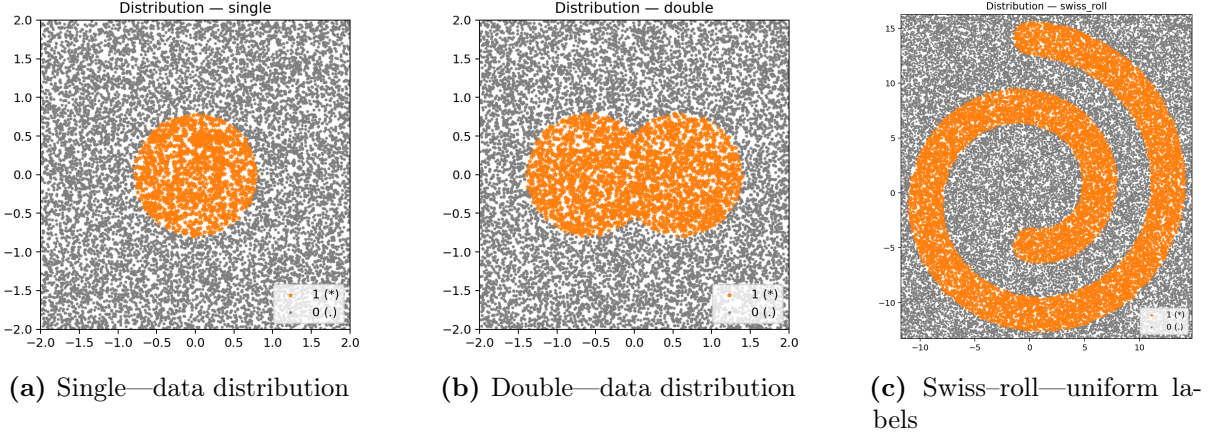


Figure 5: Distributions used in the three cases, positives are colored in orange, while negatives are in gray.

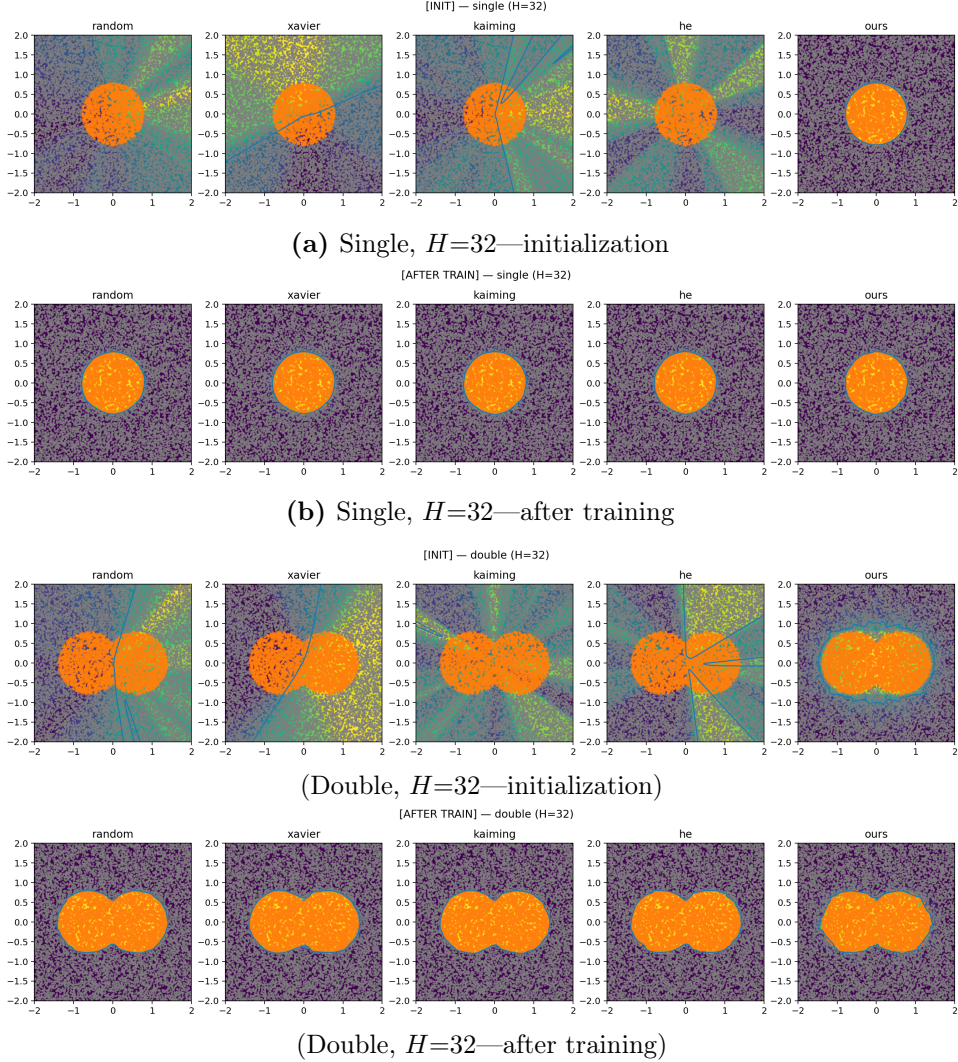


Figure 6: Decision maps for the five initializations. The blue contour line marks the 0.5 is the decision boundary ($\tau = 0.5$). The background shows the predicted probability $\sigma(z)$; warmer colors indicate higher probability (closer to 1).

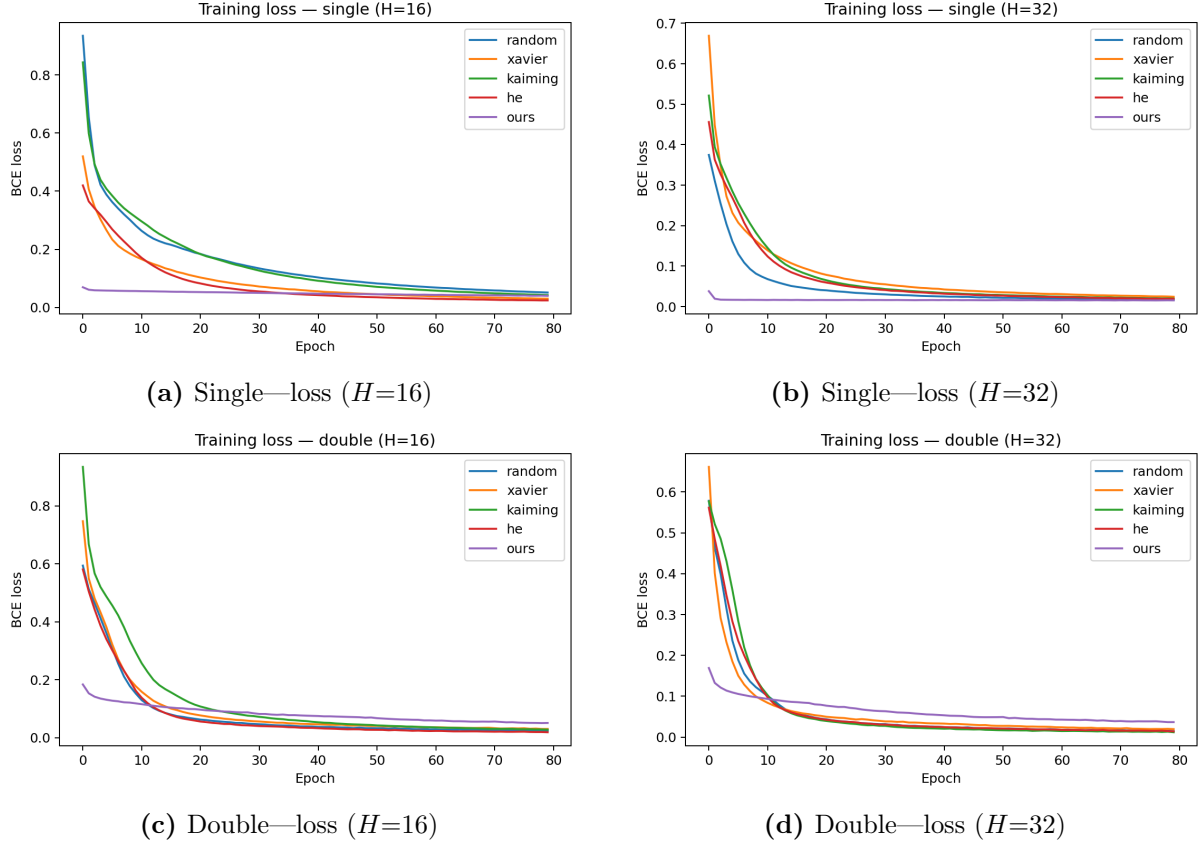


Figure 7: Training curves across initializations.

8.4 Swiss-roll

The network starts from a geometrically consistent initialization (INIT: BCE = 0.5823, Brier= 0.1615, IoU= 0.6477, AUC= 0.9336) and is then refined by training with early stopping, after which performance improves to (AFTER(early-stopped at epoch = 67: BCE = 0.0454, Brier= 0.0060, IoU= 0.9845, AUC= 0.9999). Fig. 8 shows the initialized and final probability maps, together with the loss curve.

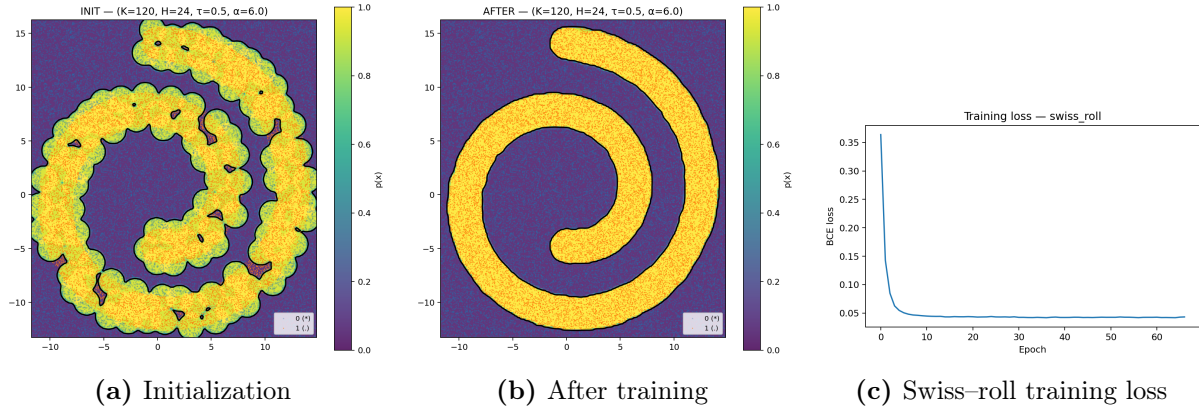


Figure 8: Swiss-roll case: geometric construction and post-training refinement.

Although our construction may seem to be artificial, the construction plays an important role in describing the inductive bias of purely sigmoidal MLPs. By compiling target geometry into sigmoidal half-space gates (Secs. 5–6), we obtain networks whose *initialized* decision boundaries

already align with the task geometry up to a narrow band. On planar numerical experiments, we observed near-perfect AUC and high IoU at initialization for the constructive models, while standard random/Xavier/Kaiming/He initializations start near chance and rely entirely on optimization and training to discover the geometric boundary.

9 Conclusions

We revisited Universal Approximation Theorem for sigmoidal Multi-Layer Perceptrons through a constructive, tropical geometry-aware sense. Within the finite-sum form (2.1), our method build a covering of the target region into sigmoidal half-space gates, yielding decision boundaries that agree with the prescribed geometry at *initialization*; subsequent optimization is not essential and primarily refines calibration rather than discovering the boundary. This positions our approach as a smooth counterpart to tropical, boundary-first reasoning while remaining entirely sigmoidal.

Limitations. Our analysis and constructions focus on planar ($d=2$) binary classification with logistic sigmoid function; while Sec. 7 gives the outlines to higher-dimensional extensions, we have not yet provided the same level of quantitative study beyond the plane. The construction algorithm depends on a reasonable covering (e.g., by disks); extremely fine geometric detail or high curvature can increase the required size of the network. Finally, although training typically preserves the intended union semantics, incorrect centering/scaling of the head can degrade stability.

Future Works. Two directions appear especially promising: (i) principled cover selection with approximation guarantees and budget-aware trade-offs; and (ii) integrating tropical certificates with sigmoidal training, e.g., enforcing margin/coverage constraints derived from support functions during optimization. More broadly, we view geometry-aware compilation as a practical bridge between classical UAT and tropical structure: it turns *where* the boundary should be (Sections 5–6) into *how* to place weights so that the MLP starts, which allow learning focus on calibration and robustness rather than boundary discovery.

References

- [1] Muhammad AlFarra, Adel Bibi, Hossein Hammoud, Mohamed Gaafar, and Bernard Ghanem. On the decision boundaries of neural networks: A tropical geometry perspective. *IEEE Transactions on Pattern Analysis and Machine Intelligence*, 44(12):9715–9728, 2022. doi: 10.1109/TPAMI.2021.3112132.
- [2] Andrew R. Barron. Universal approximation bounds for superpositions of a sigmoidal function. *IEEE Transactions on Information Theory*, 39(3):930–945, 1993. doi: 10.1109/18.256500.
- [3] Max-Christian Brandenburg, Georg Loho, and Guido Montúfar. The real tropical geometry of neural networks, 2024. URL <https://arxiv.org/abs/2403.11871>.
- [4] Glenn W. Brier. Verification of forecasts expressed in terms of probability. *Monthly Weather Review*, 78(1):1–3, 1950. doi: 10.1175/1520-0493(1950)078<0001:VOFEIT>2.0.CO;2.
- [5] George Cybenko. Approximation by superpositions of a sigmoidal function. *Mathematics of Control, Signals and Systems*, 2(4):303–314, 1989. doi: 10.1007/BF02551274.
- [6] Herbert Edelsbrunner and John Harer. *Computational Topology: An Introduction*. American Mathematical Society, 2010. See Theorem 10.7 (Nerve Theorem) and discussion of Čech complexes.

- [7] Kostas Fotopoulos, Petros Maragos, and Panos Misiakos. Tropnnnc: Structured neural network compression using tropical geometry, 2024. URL <https://arxiv.org/abs/2409.03945>.
- [8] Ken-Ichi Funahashi. On the approximate realization of continuous mappings by neural networks. *Neural Networks*, 2(3):183–192, 1989. doi: 10.1016/0893-6080(89)90003-8.
- [9] Xavier Glorot and Yoshua Bengio. Understanding the difficulty of training deep feedforward neural networks. In Yee Whye Teh and Mike Titterington, editors, *Proceedings of the Thirteenth International Conference on Artificial Intelligence and Statistics (AISTATS)*, volume 9 of *JMLR: Workshop and Conference Proceedings*, pages 249–256, 2010.
- [10] Teofilo F. Gonzalez. Clustering to minimize the maximum intercluster distance. In *Theoretical Computer Science, 5th International Conference, ICALP 1978*, pages 281–291. Springer, 1978. Often cited for the 2-approximation of the k -center problem; used here as the classic farthest-point heuristic.
- [11] James A. Hanley and Barbara J. McNeil. The meaning and use of the area under a receiver operating characteristic (roc) curve. *Radiology*, 143(1):29–36, 1982. doi: 10.1148/radiology.143.1.7063747.
- [12] Allen Hatcher. *Algebraic Topology*. Cambridge University Press, 2002. URL <https://pi.math.cornell.edu/~hatcher/AT/AT.pdf>. See Proposition 4G.3 (Nerve Lemma).
- [13] Kaiming He, Xiangyu Zhang, Shaoqing Ren, and Jian Sun. Delving deep into rectifiers: Surpassing human-level performance on imagenet classification. In *Proceedings of the IEEE International Conference on Computer Vision (ICCV)*, pages 1026–1034, 2015. doi: 10.1109/ICCV.2015.123.
- [14] Kurt Hornik. Approximation capabilities of multilayer feedforward networks. *Neural Networks*, 4(2):251–257, 1991. doi: 10.1016/0893-6080(91)90009-T.
- [15] Kurt Hornik, Maxwell Stinchcombe, and Halbert White. Multilayer feedforward networks are universal approximators. *Neural Networks*, 2(5):359–366, 1989. doi: 10.1016/0893-6080(89)90020-8.
- [16] Kurt Hornik, Maxwell Stinchcombe, and Halbert White. Universal approximation of an unknown mapping and its derivatives using multilayer feedforward networks. *Neural Networks*, 3(5):551–560, 1990. doi: 10.1016/0893-6080(90)90005-6.
- [17] Guang-Bin Huang, Qin-Yu Zhu, and Chee-Kheong Siew. Extreme learning machine: Theory and applications. *Neurocomputing*, 70(1-3):489–501, 2006. doi: 10.1016/j.neucom.2005.12.126.
- [18] Paul Jaccard. étude comparative de la distribution florale dans une portion des alpes et des jura. *Bulletin de la Société Vaudoise des Sciences Naturelles*, 37:547–579, 1901.
- [19] Diederik P. Kingma and Jimmy Ba. Adam: A method for stochastic optimization. *International Conference on Learning Representations (ICLR)*, 2015. arXiv:1412.6980.
- [20] Moshe Leshno, Vladimir Y. Lin, Allan Pinkus, and Shimon Schocken. Multilayer feedforward networks with a nonpolynomial activation function can approximate any function. *Neural Networks*, 6(6):861–867, 1993. doi: 10.1016/S0893-6080(05)80131-5.
- [21] Diane Maclagan and Bernd Sturmfels. *Introduction to Tropical Geometry*, volume 161 of *Graduate Studies in Mathematics*. American Mathematical Society, 2015. ISBN 978-0-8218-5198-2.

- [22] Leland McInnes, John Healy, and James Melville. Umap: Uniform manifold approximation and projection for dimension reduction. *arXiv preprint arXiv:1802.03426*, 2018.
- [23] Dmytro Mishkin and Jiří Matas. All you need is a good init. *arXiv preprint arXiv:1511.06422*, 2016. ICLR 2016 Workshop version.
- [24] Mona Mohnhaupt. The nerve theorem and its applications in topological data analysis. Bachelor thesis, ETH Zürich, Zürich, Switzerland, June 2023. URL https://people.math.ethz.ch/~skalisnik/theses/Mohnhaupt_Bsc.pdf. Supervisor: Sara Kališnik Hintz.
- [25] Guido F. Montúfar, Razvan Pascanu, Kyunghyun Cho, and Yoshua Bengio. On the number of linear regions of deep neural networks. In *Advances in Neural Information Processing Systems (NeurIPS)*, volume 27, pages 2924–2932, 2014.
- [26] Ralph Morrison. Tropical geometry, 2019. URL <https://arxiv.org/abs/1908.07012>. Chapter for *Foundations for Undergraduate Research in Mathematics*, 40 pp.
- [27] Partha Niyogi, Steve Smale, and Shmuel Weinberger. Finding the homology of submanifolds with high confidence from random samples. *Discrete & Computational Geometry*, 39(1-3): 419–441, 2008. doi: 10.1007/s00454-008-9053-2. Offsets of smooth compact submanifolds are homotopy equivalent to the manifold for radii below the reach.
- [28] Jooyoung Park and Irwin W. Sandberg. Universal approximation using radial-basis-function networks. *Neural Computation*, 3(2):246–257, 1991. doi: 10.1162/neco.1991.3.2.246.
- [29] Allan Pinkus. *Approximation Theory of the MLP Model in Neural Networks*. Acta Numerica, 1999. doi: 10.1017/S0962492900002919.
- [30] Matus Telgarsky. Benefits of depth in neural networks. In *Proceedings of the 29th Annual Conference on Learning Theory (COLT)*, pages 1517–1539, 2016.
- [31] Lei Zhang, Gregory Naitzat, and Lek-Heng Lim. Tropical geometry of deep neural networks. In *Proceedings of the 35th International Conference on Machine Learning (ICML)*, volume 80 of *PMLR*, pages 5824–5832, 2018. URL <https://proceedings.mlr.press/v80/zhang18i.html>.